SCA 2025

# UNFOLDING THE POWER OF GREEN'S FUNCTIONS FOR MODELING AND SIMULATION

JIONG CHEN
INRIA
08/10/2025

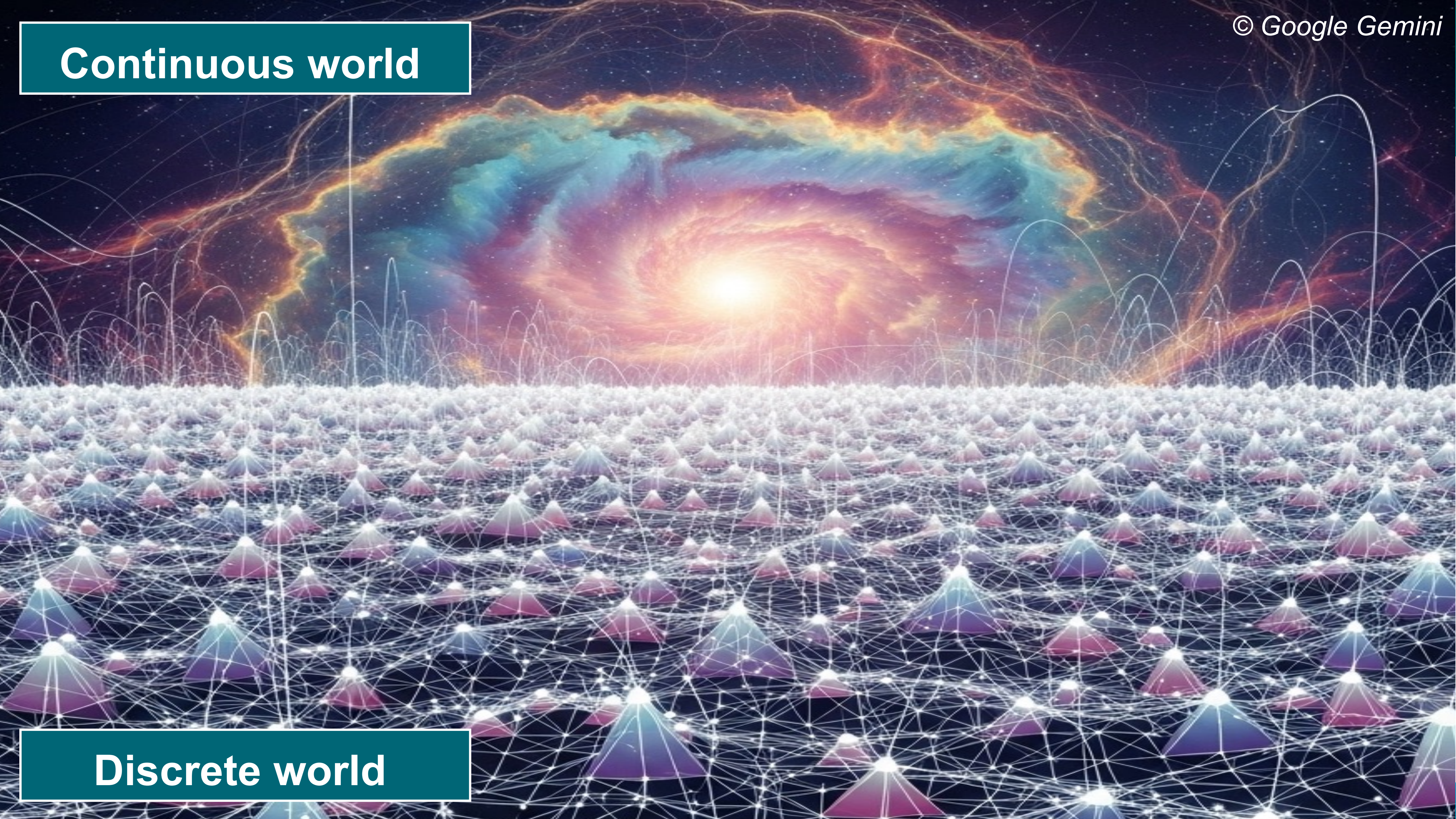
Continuous world
Discrete world

# PAST WORK ON DISCRETIZATION

***Eternal goals: high accuracy with low cost***

## FUNCTIONAL APPROXIMATION PERSPECTIVE

- Construct **hierarchical** matrix-valued basis functions & wavelets adapting to heterogeneous elasticity [Chen et al. 2018, 2019]

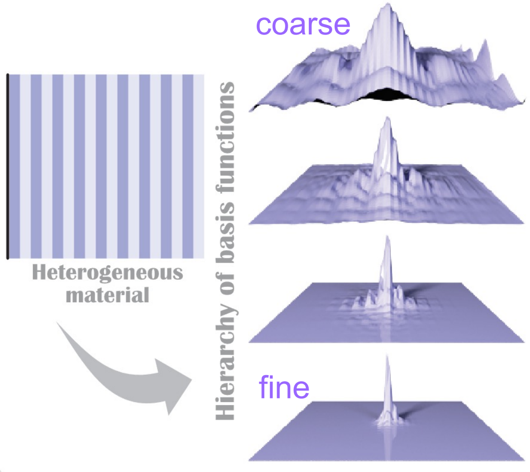


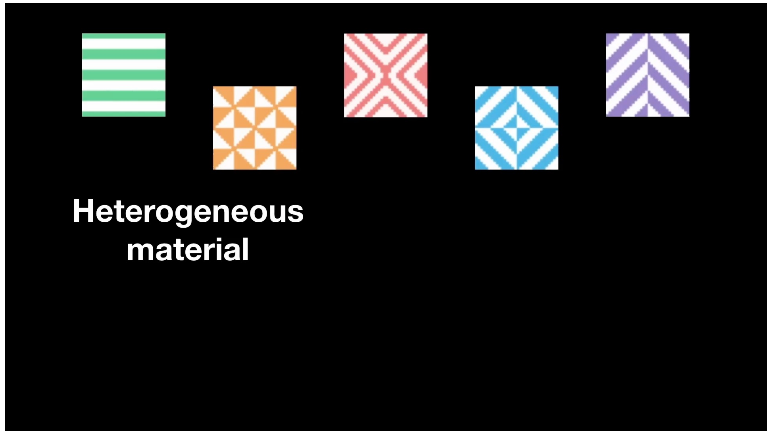


## SIGNAL SAMPLING PERSPECTIVE

- Optimize the spatial **distribution** of discrete samples by placing them where they are **most needed** [Wen et al. 2020]

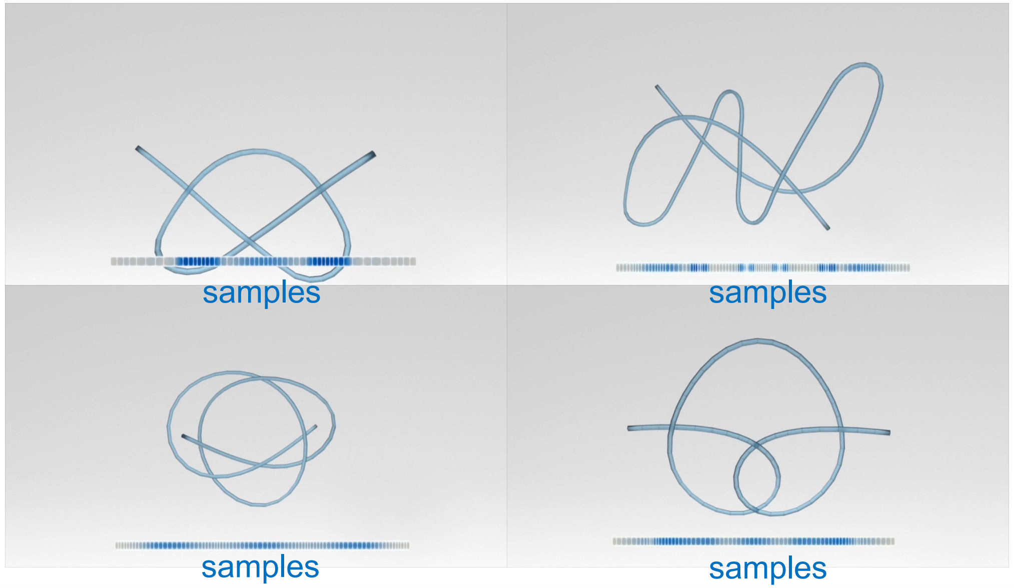

# FROM NUMERICAL TO (SEMI-) ANALYTICAL APPROACHES

SCA 2025

- Numerical approaches, e.g., FEM and FDM, are general-purpose methods…
- …but they may not fully exploit the properties of the differential operators for extreme efficiency
- The search for analytical solutions to PDEs has a much longer history than that for numerical ones
  - Led to creation of many powerful theories and tools
    - Fourier analysis, special functions, inverse scattering transform…

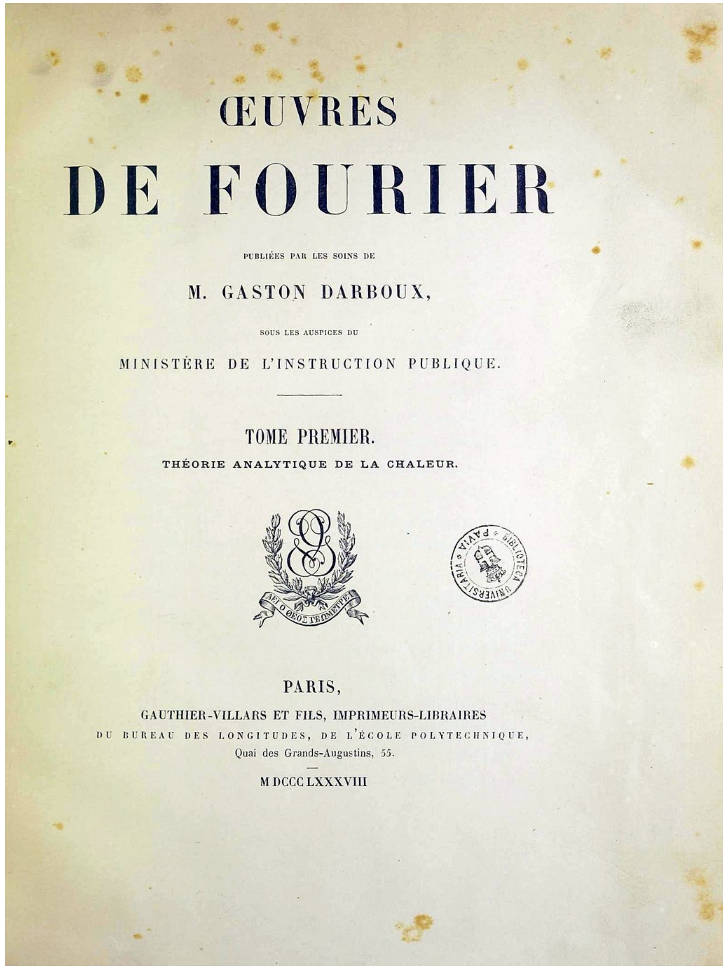


*J. Fourier, The Analytical Theory of Heat, 1888*

# FROM NUMERICAL TO (SEMI-) ANALYTICAL APPROACHES

- Numerical approaches, e.g., FEM and FDM, are general-purpose methods…
- …but they may not fully exploit the properties of the differential operators for extreme efficiency
- The search for analytical solutions to PDEs has a much longer history than that for numerical ones
  - Led to creation of many powerful theories and tools
    - Fourier analysis, special functions, inverse scattering transform…
- What can we do with analytical solutions in modeling and simulation?

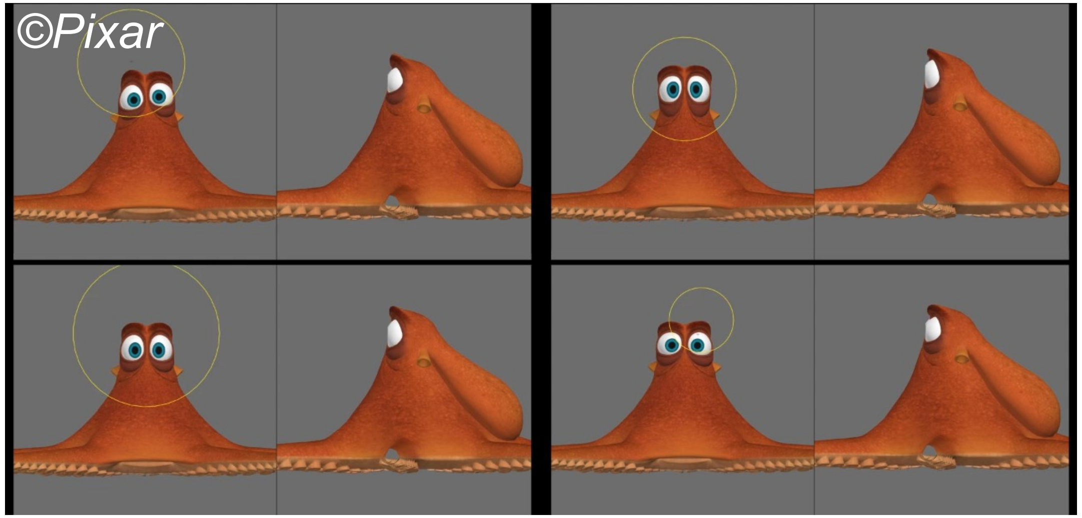


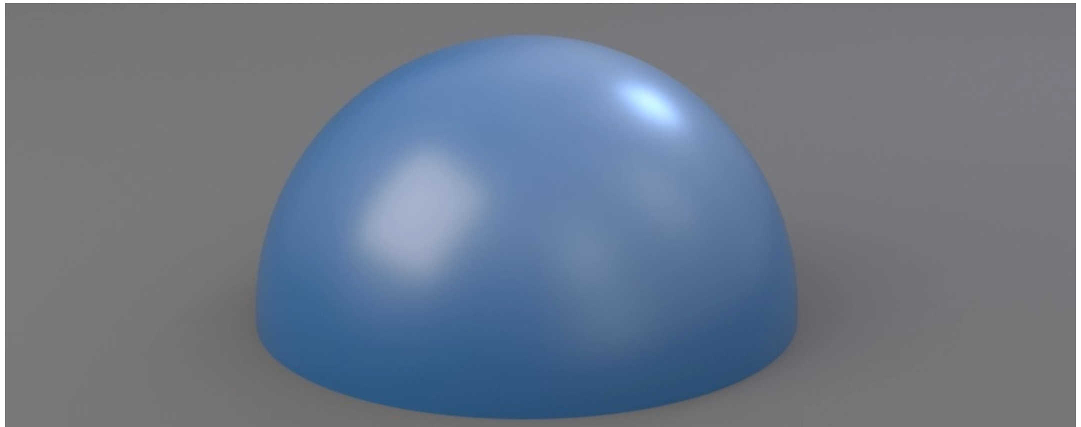

*Regularized Kelvinlets*

[de Goes and James 2017, 2018]

# METHOD OF GREEN'S FUNCTIONS

**Green's function** – **analytical** solution to **homogenous** & **"boundless"** PDEs *w.r.t.* a **singular** impulse

- Given a linear and homogeneous PDE

$$\mathcal{L}u(x) = f(x)$$

- A Green's function $G(x,s)$ is defined as

$$\mathcal{L}G(x,s) = \delta(x-s)$$

- Solution expressed via convolution

$$u(x) = \int G(x,s) f(s) \, \mathrm{d}s$$

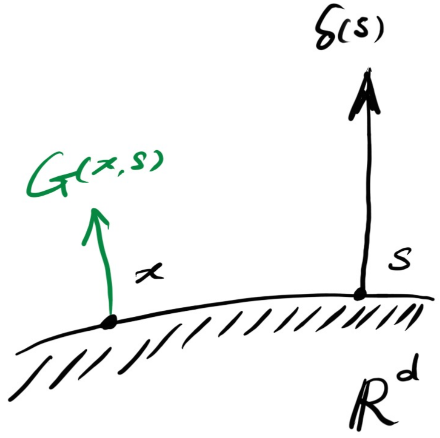


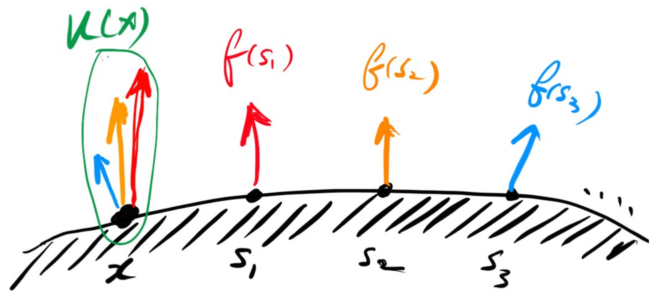


**No equation solves, cheap to evaluate!**

# METHOD OF GREEN'S FUNCTIONS



| Differential operator $L$ | Green's function $G$ | Example of application |
|---|---|---|
| $\partial_t^{n+1}$ | $\frac{t^n}{n!}\Theta(t)$ | |
| $\partial_t + \gamma$ | $\Theta(t)e^{-\gamma t}$ | |
| $(\partial_t + \gamma)^2$ | $\Theta(t)te^{-\gamma t}$ | |
| $\partial_t^2 + 2\gamma\partial_t + \omega_0^2$ where $\gamma < \omega_0$ | $\Theta(t)e^{-\gamma t}\frac{\sin(\omega t)}{\omega}$ with $\omega = \sqrt{\omega_0^2 - \gamma^2}$ | 1D underdamped harmonic oscillator |
| $\partial_t^2 + 2\gamma\partial_t + \omega_0^2$ where $\gamma > \omega_0$ | $\Theta(t)e^{-\gamma t}\frac{\sinh(\omega t)}{\omega}$ with $\omega = \sqrt{\gamma^2 - \omega_0^2}$ | 1D overdamped harmonic oscillator |
| $\partial_t^2 + 2\gamma\partial_t + \omega_0^2$ where $\gamma = \omega_0$ | $\Theta(t)e^{-\gamma t}t$ | 1D critically damped harmonic oscillator |
| 2D Laplace operator $\nabla_{2D}^2 = \partial_x^2 + \partial_y^2$ | $\frac{1}{2\pi}\ln\rho$ with $\rho = \sqrt{x^2 + y^2}$ | 2D Poisson equation |
| 3D Laplace operator $\nabla_{3D}^2 = \partial_x^2 + \partial_y^2 + \partial_z^2$ | $\frac{-1}{4\pi r}$ with $r = \sqrt{x^2 + y^2 + z^2}$ | Poisson equation |
| Helmholtz operator $\nabla_{3D}^2 + k^2$ | $\frac{-e^{-ikr}}{4\pi r} = i\sqrt{\frac{k}{32\pi r}}H_{1/2}^{(2)}(kr) = i\frac{k}{4\pi}h_0^{(2)}(kr)$ | stationary 3D Schrödinger equation for free particle |
| $\nabla^2 - k^2$ in $n$ dimensions | $-(2\pi)^{-n/2}\left(\frac{k}{r}\right)^{n/2-1}K_{n/2-1}(kr)$ | Yukawa potential, Feynman propagator |
| $\partial_t^2 - c^2\partial_x^2$ | $\frac{1}{2c}\Theta(t - \lvert x/c\rvert)$ | 1D wave equation |
| $\partial_t^2 - c^2\nabla_{2D}^2$ | $\frac{1}{2\pi c\sqrt{c^2t^2 - \rho^2}}\Theta(t - \rho/c)$ | 2D wave equation |
| D'Alembert operator $\square = \frac{1}{c^2}\partial_t^2 - \nabla_{3D}^2$ | $\frac{\delta(t - \frac{r}{c})}{4\pi r}$ | 3D wave equation |
| $\partial_t - k\partial_x^2$ | $\Theta(t)\left(\frac{1}{4\pi kt}\right)^{1/2}e^{-x^2/4kt}$ | 1D diffusion |
| $\partial_t - k\nabla_{2D}^2$ | $\Theta(t)\left(\frac{1}{4\pi kt}\right)e^{-\rho^2/4kt}$ | 2D diffusion |
| $\partial_t - k\nabla_{3D}^2$ | $\Theta(t)\left(\frac{1}{4\pi kt}\right)^{3/2}e^{-r^2/4kt}$ | 3D diffusion |
| $\frac{1}{c^2}\partial_t^2 - \partial_x^2 + \mu^2$ | $\frac{1}{2}[(1 - \sin\mu ct)(\delta(ct - x) + \delta(ct + x)) + \mu\Theta(ct - \lvert x\rvert)J_0(\mu u)]$ with $u = \sqrt{c^2t^2 - x^2}$ | 1D Klein–Gordon equation |
| $\frac{1}{c^2}\partial_t^2 - \nabla_{2D}^2 + \mu^2$ | $\frac{1}{4\pi}\left[(1 + \cos(\mu ct))\frac{\delta(ct - \rho)}{\rho} + \mu^2\Theta(ct - \rho)\,\mathrm{sinc}(\mu u)\right]$ with $u = \sqrt{c^2t^2 - \rho^2}$ | 2D Klein–Gordon equation |
| $\square + \mu^2$ | $\frac{1}{4\pi}\left[\frac{\delta\left(t - \frac{r}{c}\right)}{r} + \mu c\Theta(ct - r)\frac{J_1(\mu u)}{u}\right]$ with $u = \sqrt{c^2t^2 - r^2}$ | 3D Klein–Gordon equation |
| $\partial_t^2 + 2\gamma\partial_t - c^2\partial_x^2$ | $\frac{1}{2}e^{-\gamma t}\left[\delta(ct - x) + \delta(ct + x) + \Theta(ct - \lvert x\rvert)\left(\frac{\gamma}{c}I_0\left(\frac{\gamma u}{c}\right) + \frac{\gamma t}{u}I_1\left(\frac{\gamma u}{c}\right)\right)\right]$ with $u = \sqrt{c^2t^2 - x^2}$ | telegrapher's equation |
| $\partial_t^2 + 2\gamma\partial_t - c^2\nabla_{2D}^2$ | $\frac{e^{-\gamma t}}{4\pi}\left[(1 + e^{-\gamma t} + 3\gamma t)\frac{\delta(ct - \rho)}{\rho} + \Theta(ct - \rho)\left(\frac{\gamma\sinh\left(\frac{\gamma u}{c}\right)}{cu} + \frac{3\gamma t\cosh\left(\frac{\gamma u}{c}\right)}{u^2} - \frac{3ct\sinh\left(\frac{\gamma u}{c}\right)}{u^3}\right)\right]$ with $u = \sqrt{c^2t^2 - \rho^2}$ | 2D relativistic heat conduction |
| $\partial_t^2 + 2\gamma\partial_t - c^2\nabla_{3D}^2$ | $\frac{e^{-\gamma t}}{20\pi}\left[(8 - 3e^{-\gamma t} + 2\gamma t + 4\gamma^2t^2)\frac{\delta(ct - r)}{r^2} + \frac{\gamma^2}{c}\Theta(ct - r)\left(\frac{1}{cu}I_1\left(\frac{\gamma u}{c}\right) + \frac{4t}{u^2}I_2\left(\frac{\gamma u}{c}\right)\right)\right]$ with $u = \sqrt{c^2t^2 - r^2}$ | 3D relativistic heat conduction |

Incapable of representing anisotropy

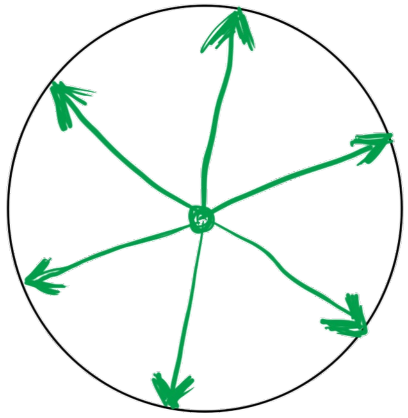

Singular at the origin

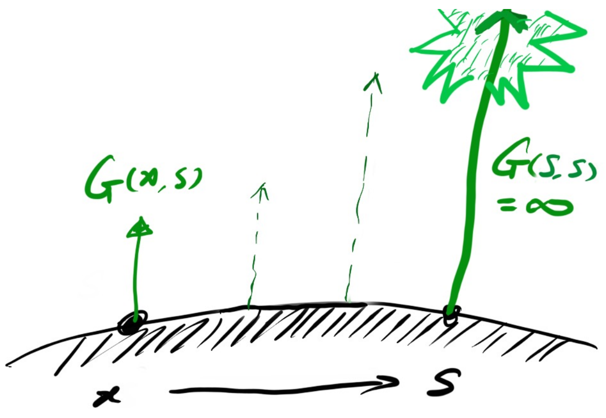

# ENFORCING BOUNDARY CONDITIONS

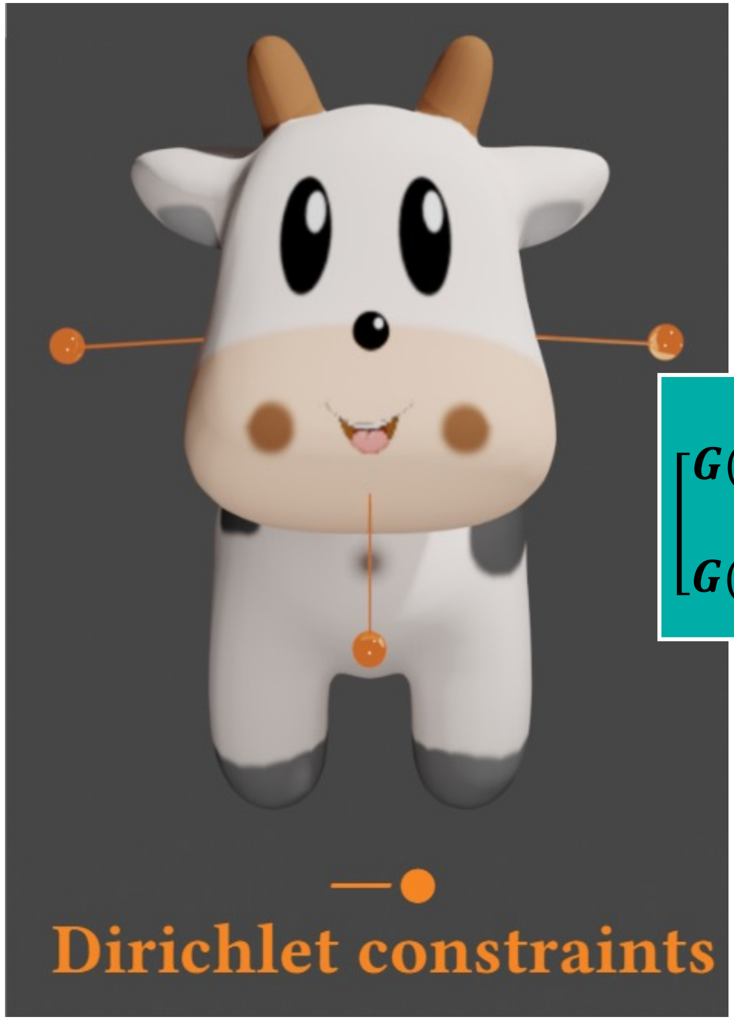


Dense linear system

$$\begin{bmatrix} G(x,x) & \cdots & G(x,y) \\ \vdots & \ddots & \vdots \\ G(y,x) & \cdots & G(y,y) \end{bmatrix} \begin{bmatrix} b_x \\ \vdots \\ b_y \end{bmatrix} = \begin{bmatrix} u_x \\ \vdots \\ u_y \end{bmatrix}$$

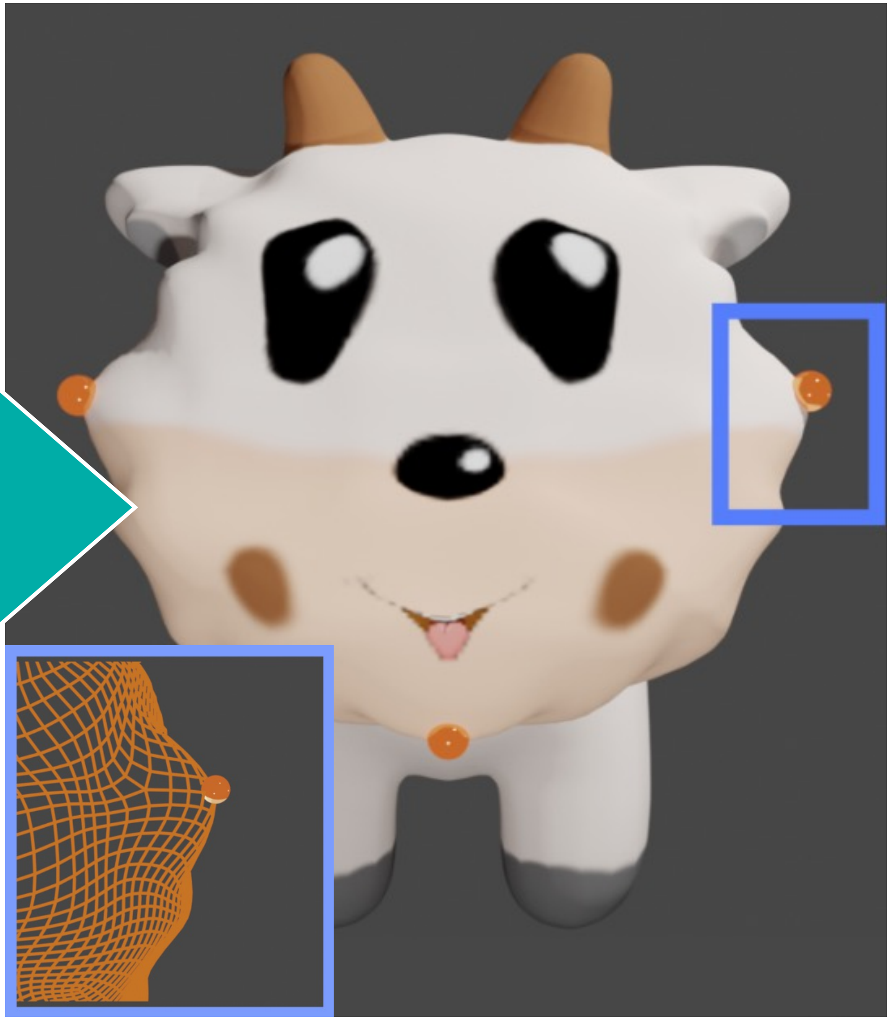

# BOUNDARY ELEMENT METHOD


# BOUNDARY ELEMENT METHOD

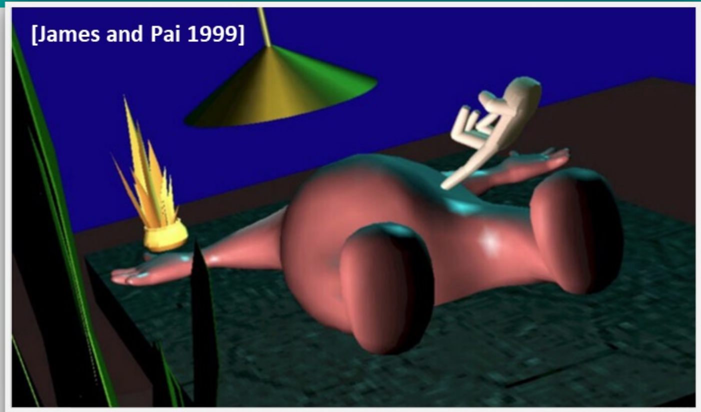


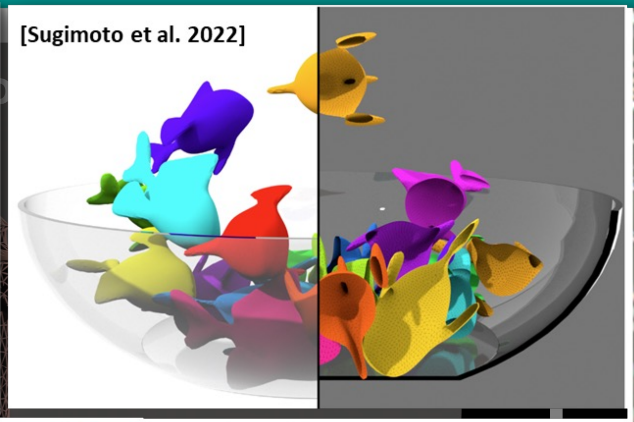



Extrapolate solutions
boundary data

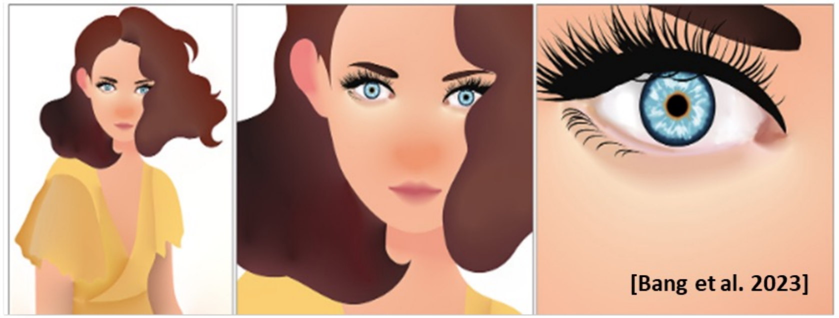


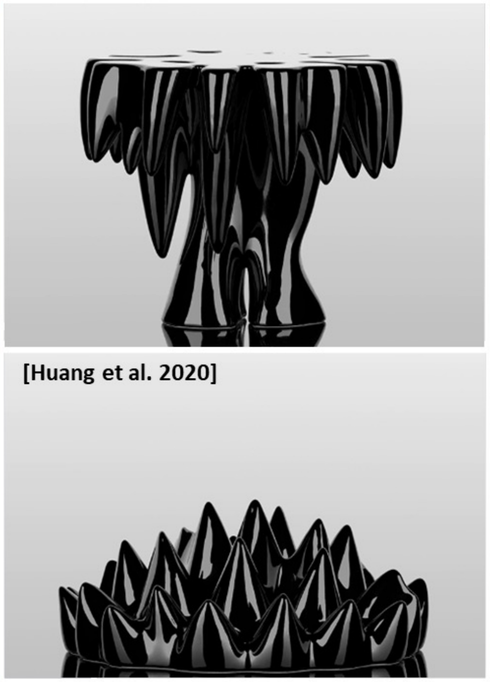


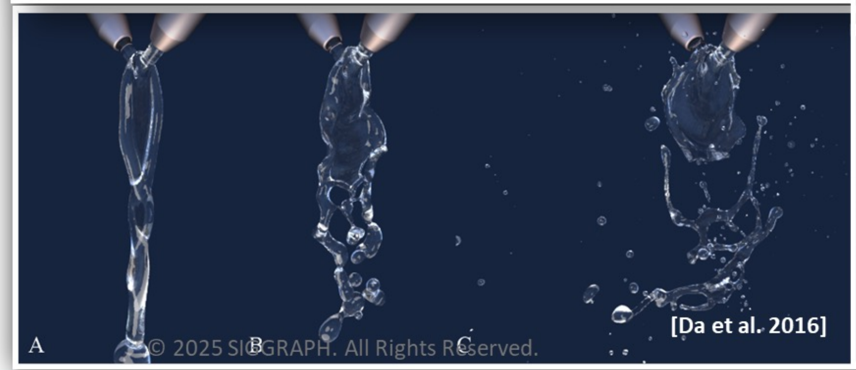



**Notoriously hard to scale up!**

# THE TWO CHALLENGES

Solve modeling/simulation problems using the method of Green's functions

$$u(x) = \int G(y,x)g(y)dS_y$$

**GENERALIZABILITY** to a wider range of linear operators and impulses

$$s.t. \ \mathcal{D}(u)|_{\partial\Omega} = u_0$$

**SCALABILITY** of enforcing boundary conditions for large-scale problems

## Applications

### Free-space shape editing

*SIGGRAPH '22*

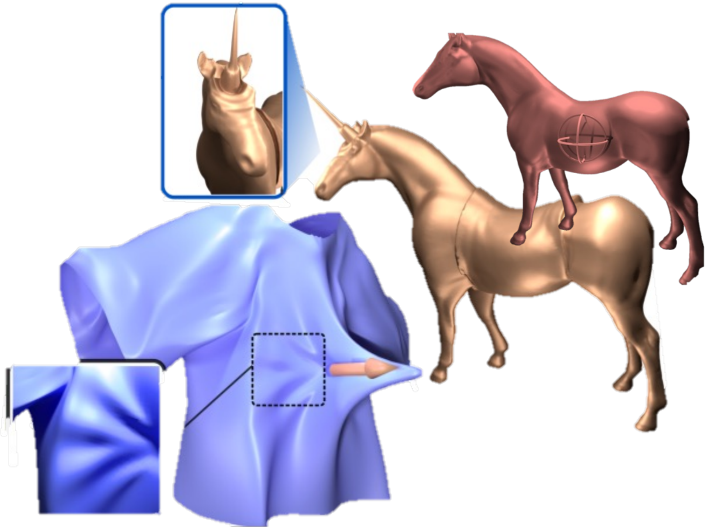

- **Mathematical tool**
  - **Fourier analysis** and **series expansion** for generalized, regularized Green's functions
- **Tradeoff**
  - No equations solves, **real-time performance**
  - **Not aware** of any boundaries

# APPROACHING THE CHALLENGES

SCA2025

## Applications

### Free-space shape editing

*SIGGRAPH ’22*

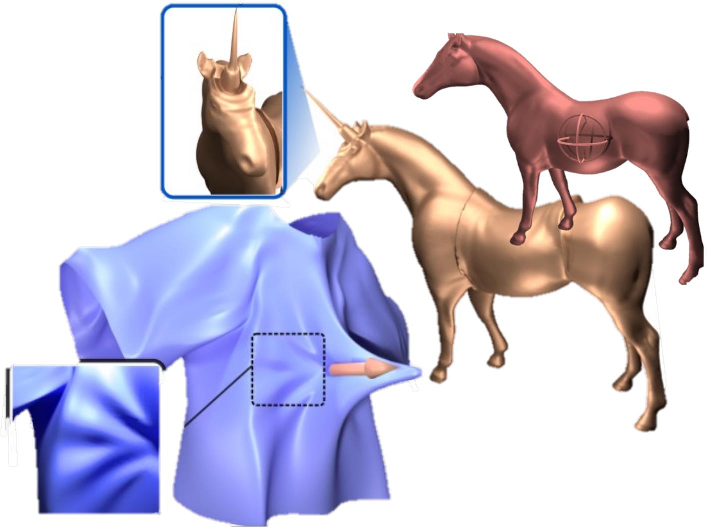

- **Mathematical tool**
  - **Fourier analysis** and **series expansion** for generalized, regularized Green’s functions
- **Tradeoff**
  - No equations solves, **real-time performance**
  - **Not aware** of any boundaries

### Scalable solvers for BIEs

*SIGGRAPH ’24 ’25*

- **Mathematical tool**
  - **Inverse matrix factorization** for preconditioning Krylov subspace iterations
- **Tradeoff**
  - Not real-time due to solving **dense systems**
  - Boundary conditions are **strictly** satisfied in a **scalable** manner

# APPROACHING THE CHALLENGES

SCA 2025

## Applications

### Free-space shape editing

*SIGGRAPH ’22*

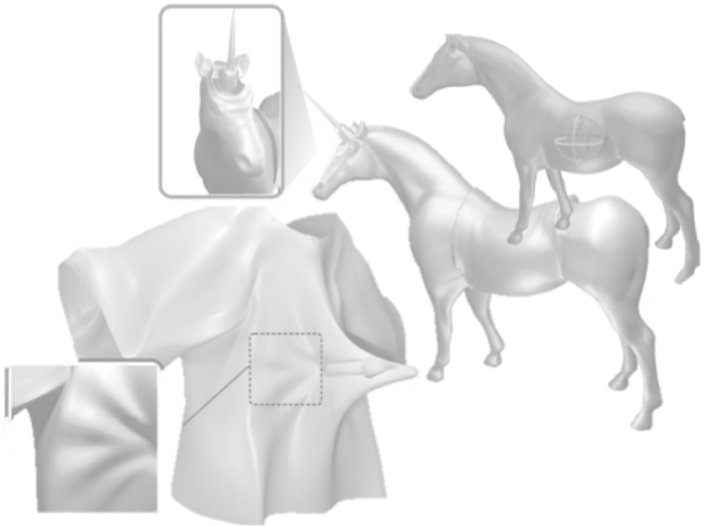

- **Mathematical tool**
  - **Fourier analysis** and **series expansion** for generalized, regularized Green’s functions
- **Tradeoff**
  - No equations solves, **real-time performance**
  - **Not aware** of any boundaries

### Cage controlled deformation tools

*SIGGRAPH ’23 ’24*

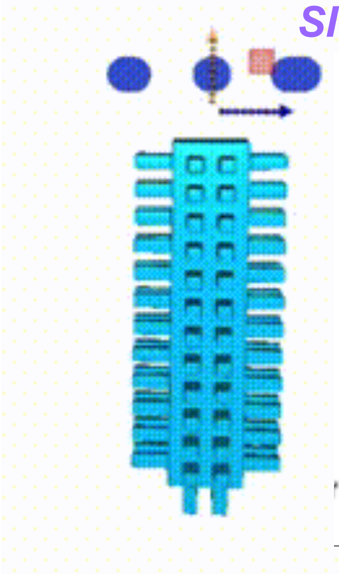

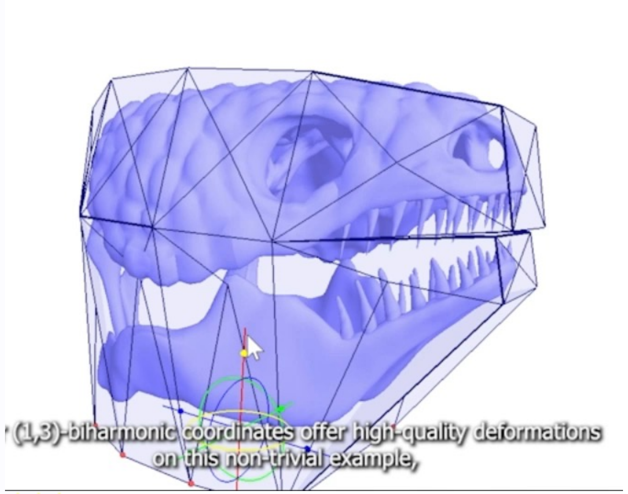


- **Mathematical tool**
  - **Generalized barycentric coordinates** w.r.t. the controlling cage
- **Tradeoff**
  - Some precomputation, **no equations solves, real-time performance**
  - Aware of boundary conditions, but only **approximately** fulfill them

### Scalable solvers for BIEs

*SIGGRAPH ’24 ’25*

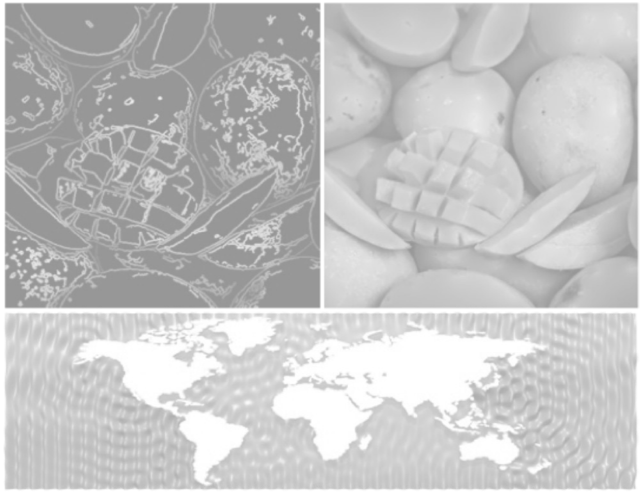

- **Mathematical tool**
  - **Inverse matrix factorization** for preconditioning Krylov subspace iterations
- **Tradeoff**
  - Not real-time due to solving **dense systems**
  - Boundary conditions are **strictly** satisfied in a **scalable** manner

# GENERALIZED GREEN'S FUNCTIONS

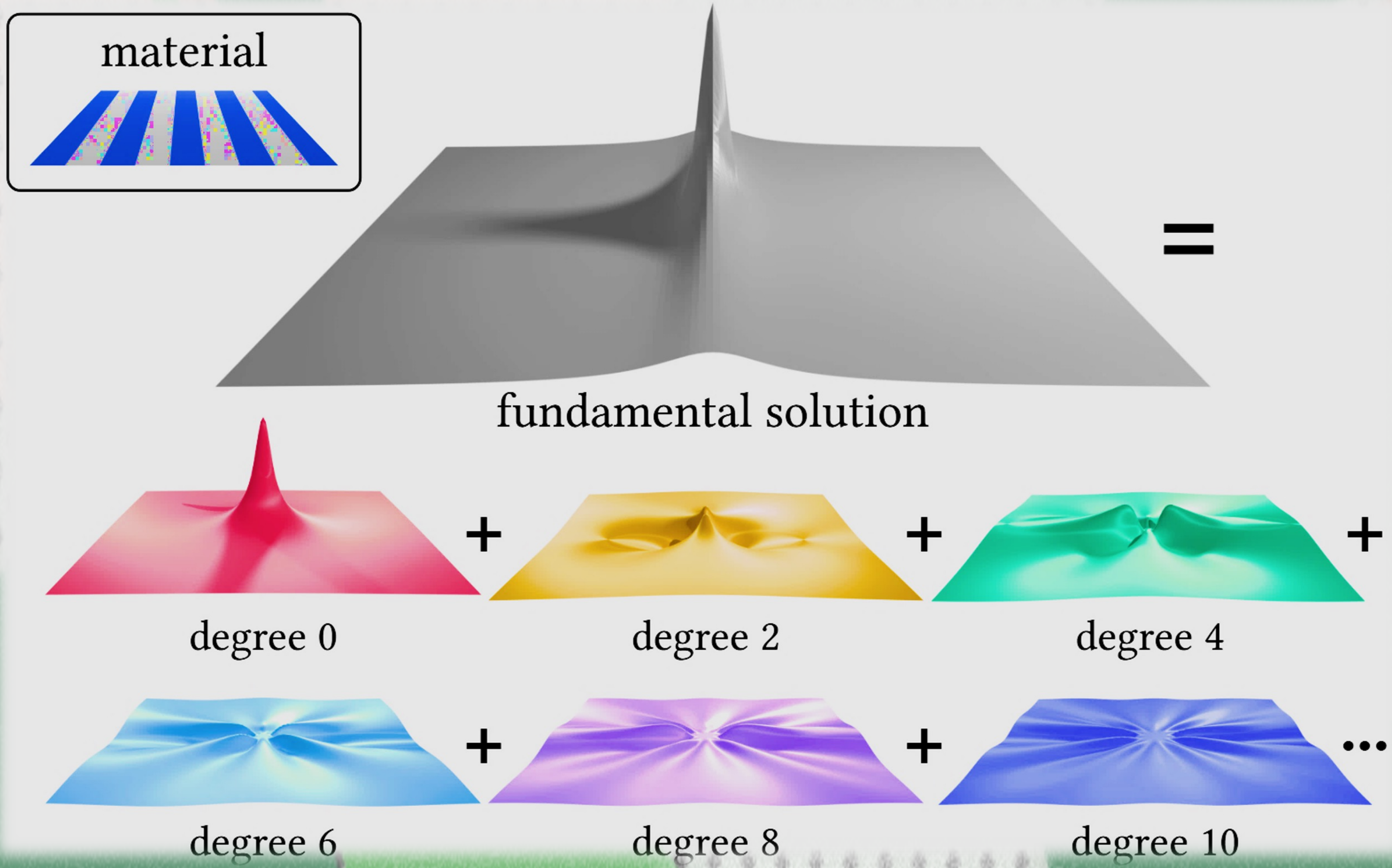

# OUR MOTIVATION

Extend Green's function to support…

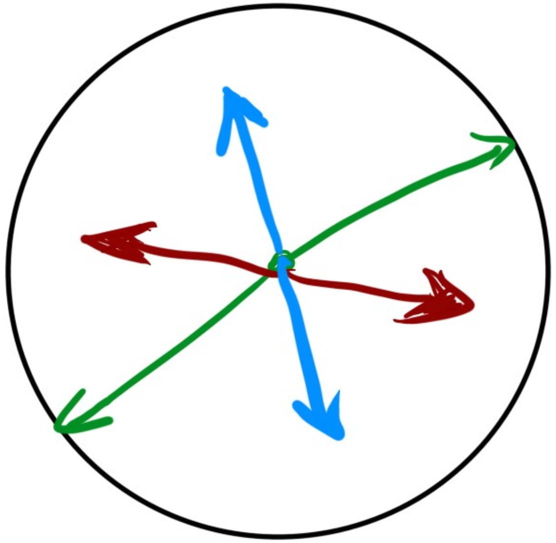

Anisotropy

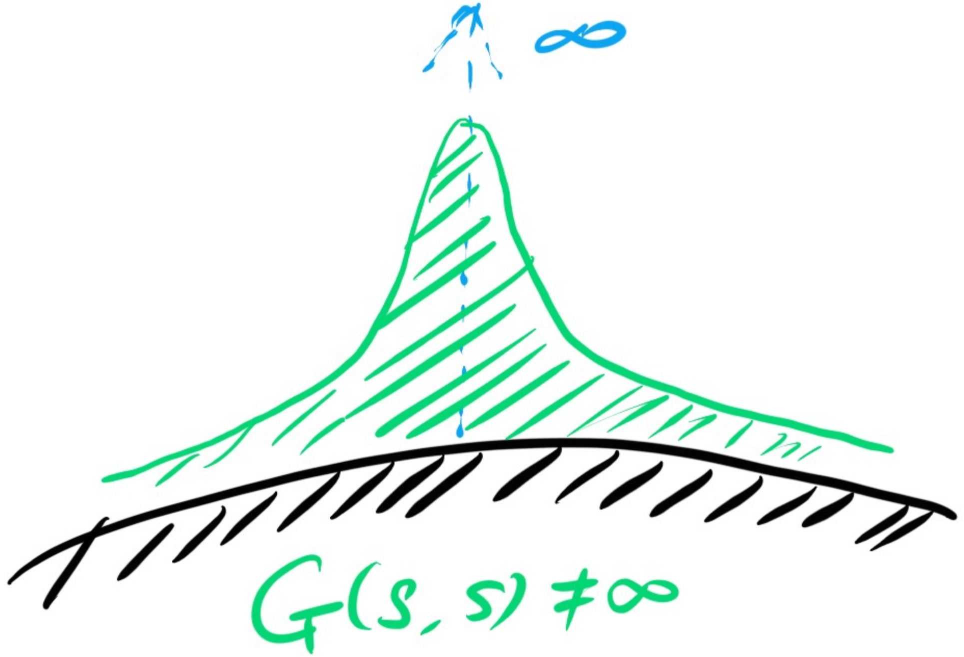


Arbitrary regularization

# GENERALIZED GREEN'S FUNCTION OF ELASTICITY

SCA2025

- **GF** to elasticity equation satisfies

$$C_{ijkl}\frac{\partial^2 G_{km}}{\partial x_l \partial x_j} + \delta_{im} g_\varepsilon(\mathbf{x}) = 0,$$

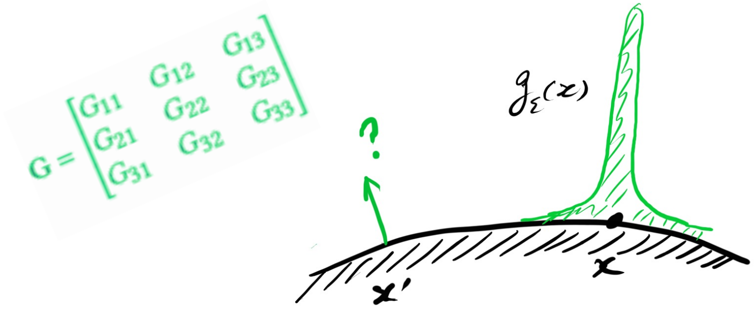


**Material $C_{ijkl}$**

Isotropic

Anisotropic

**Impulse $g_\epsilon(x)$**

$$g_\varepsilon(\mathbf{x}) = \delta(\mathbf{x})$$

$$g_\varepsilon(r) = 15\varepsilon^4/(8\pi)(r^2+\varepsilon^2)^{-\frac{7}{2}}$$

$g_\epsilon(x)$ is a more general radially symmetric function

**Green's functions**

$$\boldsymbol{u}(\boldsymbol{r}) = \left[\frac{(a-b)}{r}\boldsymbol{I} + \frac{b}{r^3}\boldsymbol{r}\boldsymbol{r}^t\right]\boldsymbol{f}$$

[Kelvin 1848]

$$\boldsymbol{u}_\varepsilon(\boldsymbol{r}) = \left[\frac{(a-b)}{r_\varepsilon}\boldsymbol{I} + \frac{b}{r_\varepsilon^3}\boldsymbol{r}\boldsymbol{r}^t + \frac{a}{2}\frac{\varepsilon^2}{r_\varepsilon^3}\boldsymbol{I}\right]\boldsymbol{f} \equiv \mathcal{K}_\varepsilon(\boldsymbol{r})\boldsymbol{f}.$$

[Cortez 2001; de Goes 2017]

???

# DERIVING GF THROUGH FOURIER TRANSFORM



- For arbitrary material and impulses, $\mathbf{G}(\mathbf{x})$ has no analytical expressions in general
- Inverse Fourier transform

$$\widehat{G}_{km}(\xi) = (C_{ijkl}\xi_l\xi_j)^{-1}\delta_{im}\widehat{g}_\varepsilon(\xi).$$

$$\mathbf{G}(\mathbf{x}) = \frac{1}{8\pi^3}\int_{\mathbb{R}^3} \widehat{\mathbf{G}}(\boldsymbol{\xi}) \exp(\mathbb{i}\,\mathbf{x}\cdot\boldsymbol{\xi})\,\mathrm{d}\boldsymbol{\xi},$$

- Plane-wave expansion, or Rayleigh expansion

$$\exp(\mathbb{i}\,\mathbf{x}\cdot\boldsymbol{\xi}) = 4\pi\sum_{l=0}^{\infty}\sum_{m=-l}^{l}\mathbb{i}^l j_l(|\mathbf{x}||\boldsymbol{\xi}|)Y_l^m(\widetilde{\mathbf{x}})\overline{Y}_l^m(\widetilde{\boldsymbol{\xi}}),$$

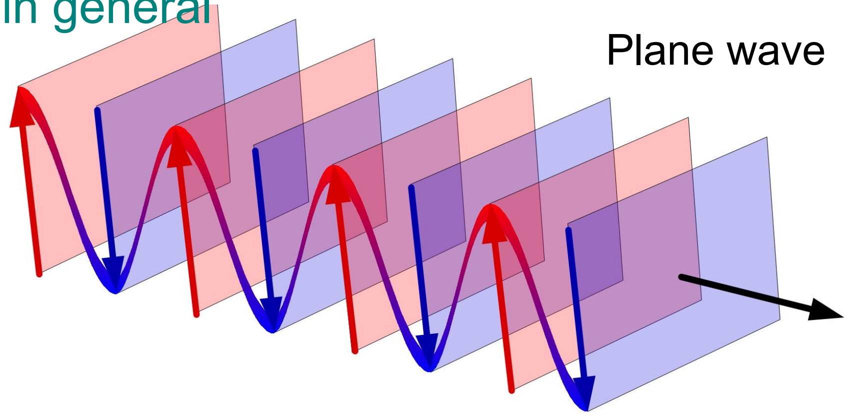

Plane wave

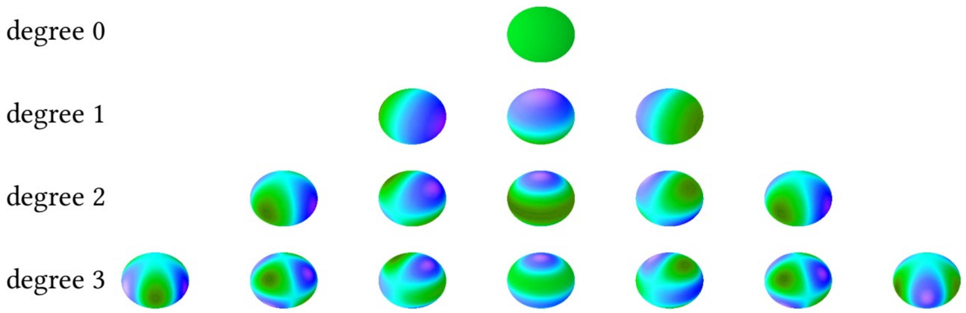


Spherical harmonics

# DERIVING GF THROUGH FOURIER TRANSFORM

SCA 2025

- For arbitrary material and impulses, $\mathbf{G}(\mathbf{x})$ has no analytical expressions in general
- Inverse Fourier transform

$$\widehat{G}_{km}(\xi) = (C_{ijkl}\xi_l\xi_j)^{-1}\delta_{im}\widehat{g}_\varepsilon(\xi).$$

$$\mathbf{G}(\mathbf{x}) = \frac{1}{8\pi^3}\int_{\mathbb{R}^3}\widehat{\mathbf{G}}(\boldsymbol{\xi})\exp(\mathbb{i}\,\mathbf{x}\cdot\boldsymbol{\xi})\,\mathrm{d}\boldsymbol{\xi},$$

- Plane-wave expansion, or Rayleigh expansion

$$\mathbf{G}(\mathbf{x}) = \frac{1}{2\pi^2}\sum_{l=0}^{\infty}\sum_{m=-l}^{l}\mathbb{i}^l\,Y_l^m(\widetilde{\mathbf{x}})\int_0^\infty \widehat{g}_\varepsilon(|\boldsymbol{\xi}|)\,j_l(|\mathbf{x}||\boldsymbol{\xi}|)\,\mathrm{d}|\boldsymbol{\xi}|\cdot \int_{\mathbb{S}^2}(C_{ikjl}\widetilde{\xi}_k\widetilde{\xi}_l)^{-1}\overline{Y_l^m}(\widetilde{\boldsymbol{\xi}})\,\mathrm{d}\mathbb{S}(\widetilde{\boldsymbol{\xi}}),$$

Plane wave

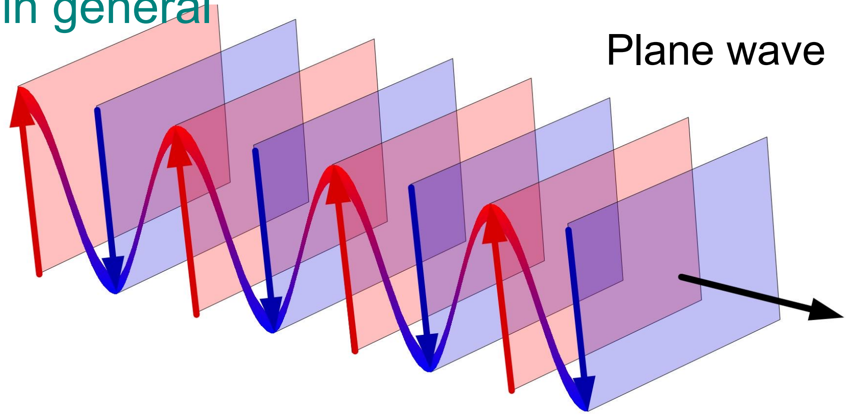

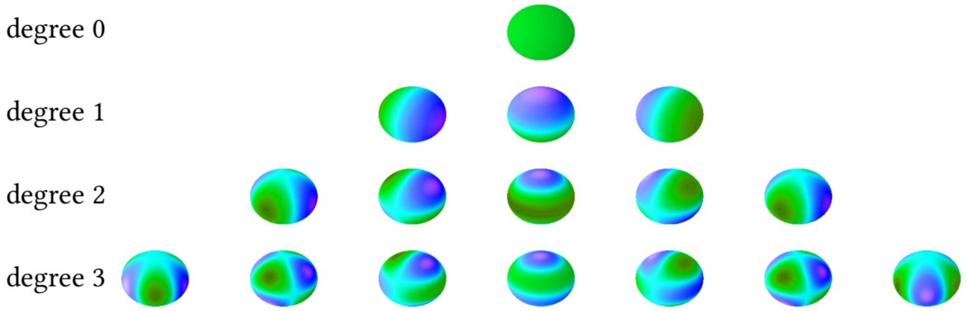


Spherical harmonics

# GREEN'S FUNCTION IN SERIES

- Expressed in spherical coordinates, $\mathbf{G}(\mathbf{x})$ is decomposed as

Directional term

Radial term

$$\int_0^\infty \widehat{g}_\varepsilon(|\xi|) j_l(|\mathbf{x}||\xi|)\,\mathrm{d}|\xi|$$

$$\mathbf{G}(r,\theta,\varphi) = \frac{1}{2\pi^2} \sum_{l=0}^{\infty} \sum_{m=-l}^{l} \mathbb{i}^l\, Y_l^m(\theta,\varphi)\, R_l(r)\, \mathbf{P}_l^m(\mathbf{C}),$$

$$\int_{\mathbb{S}^2} (C_{ikjl}\widetilde{\xi}_k\widetilde{\xi}_l)^{-1}\overline{Y}_l^m(\widetilde{\xi})\,\mathrm{d}\mathbb{S}(\widetilde{\xi})$$

Material term

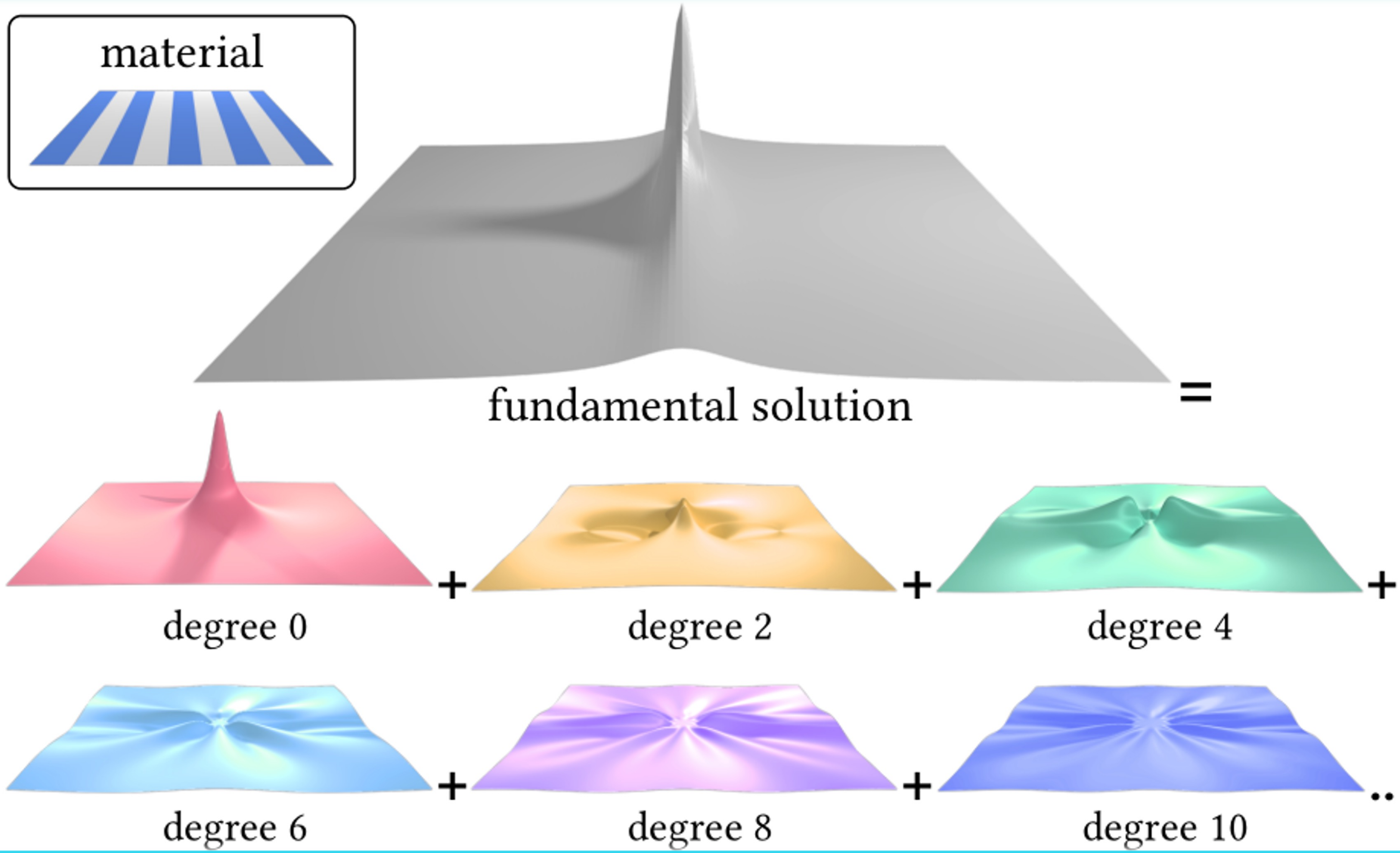
material
fundamental solution
=
degree 0
+
degree 2
+
degree 4
+
degree 6
+
degree 8
+
degree 10

# EXTENSION TO GRADIENT

- Fourier transform of partial derivative

$$\widehat{G_{ij,p}} = \mathrm{i}\,\xi_p\,\widehat{G}_{ij}, \quad p=0,1,2,$$

$$\mathcal{R}_l(|\mathbf{x}|) = \int_0^\infty \widehat{g}_\varepsilon(|\xi|)\, j_l(|\mathbf{x}||\xi|)\,|\xi|\,\mathrm{d}|\xi|,$$

- SH expansion of gradient

$$\mathcal{P}^m_{l,p}(\mathbf{C}) = \int_{\mathbb{S}^2} (C_{ikjl}\tilde{\xi}_k\tilde{\xi}_l)^{-1}\,\overline{Y}^m_l(\tilde{\xi})\,\tilde{\xi}_p\,\mathrm{d}\mathbb{S}(\tilde{\xi}).$$

$$\nabla_p \mathbf{G}(\mathbf{x}) = \frac{1}{2\pi^2}\sum_{l=0}^{\infty}\sum_{m=-l}^{l} \mathrm{i}^{l+1}\, Y_l^m(\tilde{\mathbf{x}})\,\mathcal{R}_l(|\mathbf{x}|)\,\mathcal{P}^m_{l,p}(\mathbf{C})$$

- Then given an affine load $F(x) = \delta(x - x')H$

$$\mathbf{u}(\mathbf{x}) = \mathrm{Re}\left[\nabla\mathbf{G}(\mathbf{x} - \mathbf{x}')\right] : \mathbf{H},$$

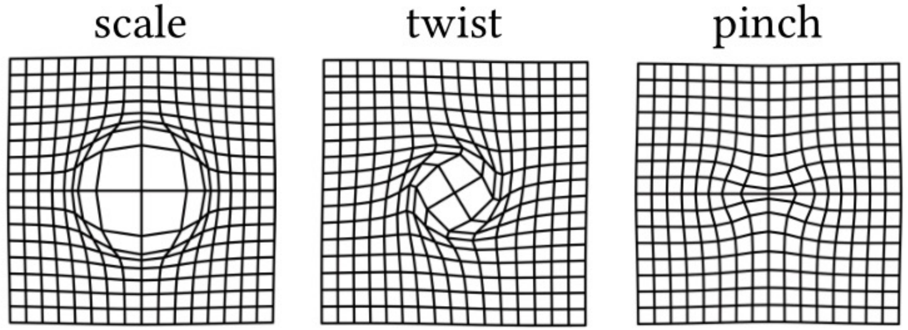

# ANISOTROPY CONTROL

- Specify an orthotropic material with 3 Young’s moduli, 3 shear moduli and 3 Poisson ratios

$$\mathbf{S}^{V}_{\text{orth}} = \begin{bmatrix} \frac{1}{E_x} & -\frac{\nu_{yx}}{E_y} & -\frac{\nu_{zx}}{E_z} & 0 & 0 & 0 \\ -\frac{\nu_{xy}}{E_x} & \frac{1}{E_y} & -\frac{\nu_{zy}}{E_z} & 0 & 0 & 0 \\ -\frac{\nu_{xz}}{E_x} & -\frac{\nu_{yz}}{E_y} & \frac{1}{E_z} & 0 & 0 & 0 \\ 0 & 0 & 0 & \frac{1}{G_{yz}} & 0 & 0 \\ 0 & 0 & 0 & 0 & \frac{1}{G_{zx}} & 0 \\ 0 & 0 & 0 & 0 & 0 & \frac{1}{G_{xy}} \end{bmatrix},$$

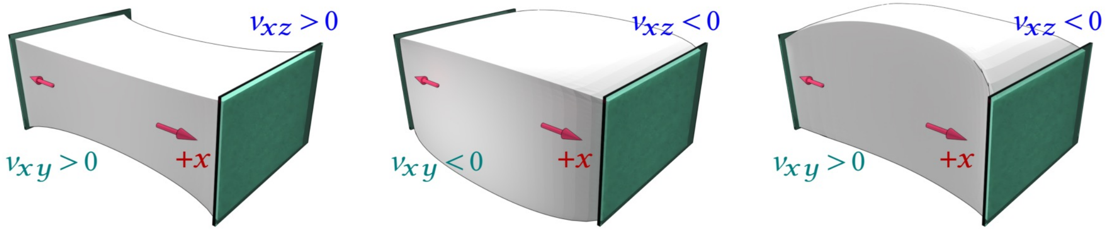


- Homogenize bi-materials on a regular grid [Kharevych et al. 2008]

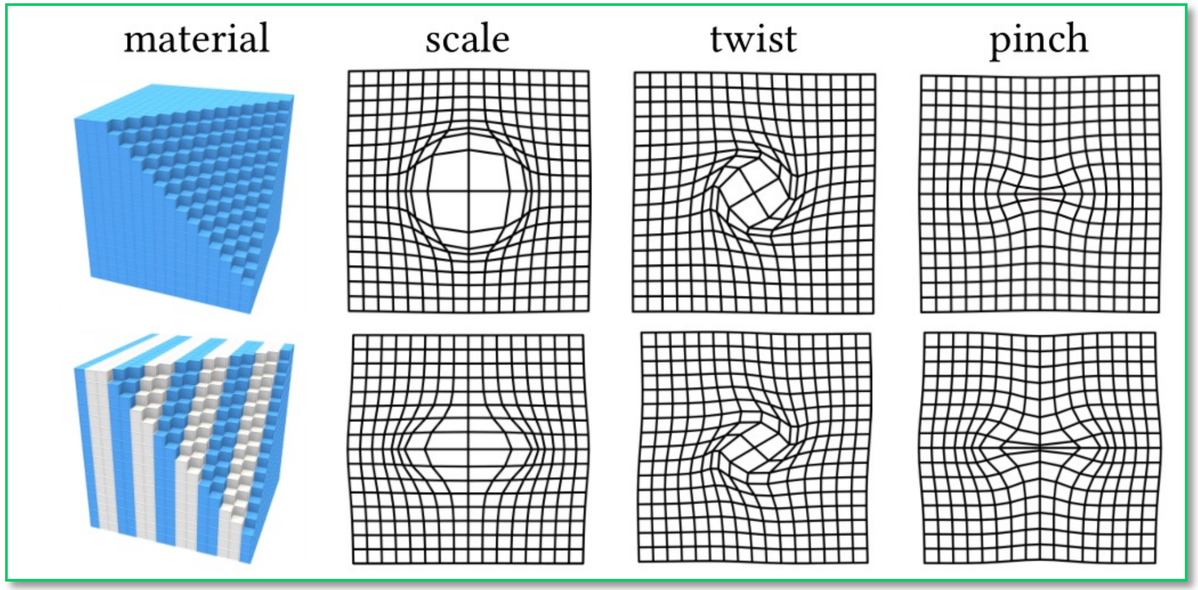


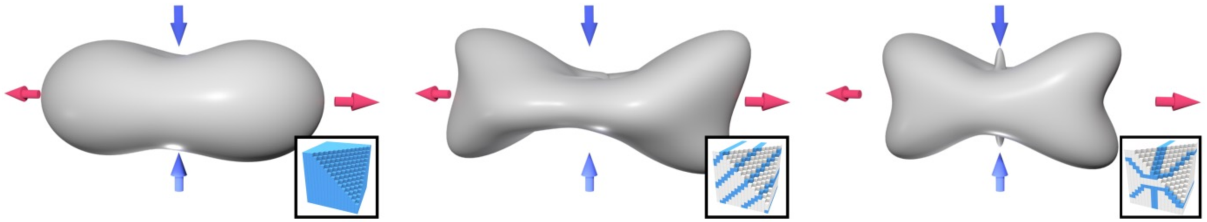

# DEFORMATION PROPAGATION CONTROL

- **Specifying the impulse function $g_\epsilon(r)$**
  - Neither intuitive nor flexible to control
  - the integral $R_l(r)$ (or $\mathcal{R}_l(r)$) is hard to evaluate for given $g_\epsilon(r)$
    - may not even exist!

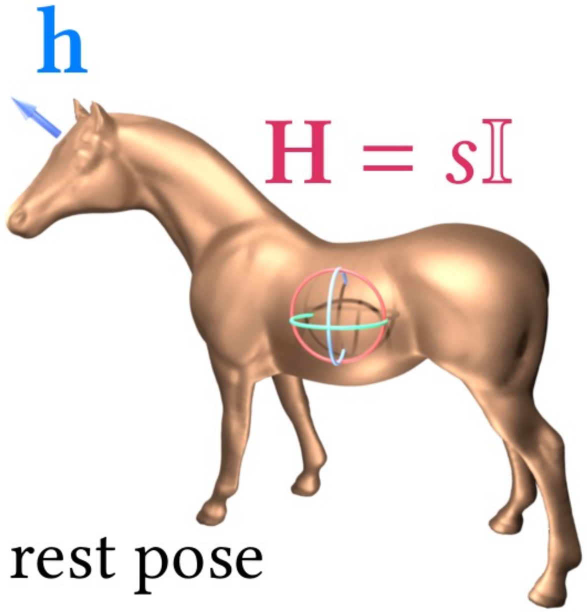


A vector load on the head
A matrix load on the belly

- **Our approach**:
  - Edit $R_l(r)$ (or $\mathcal{R}_l(r)$) directly via cubic splines instead of constructing an integrable $g_\epsilon(r)$

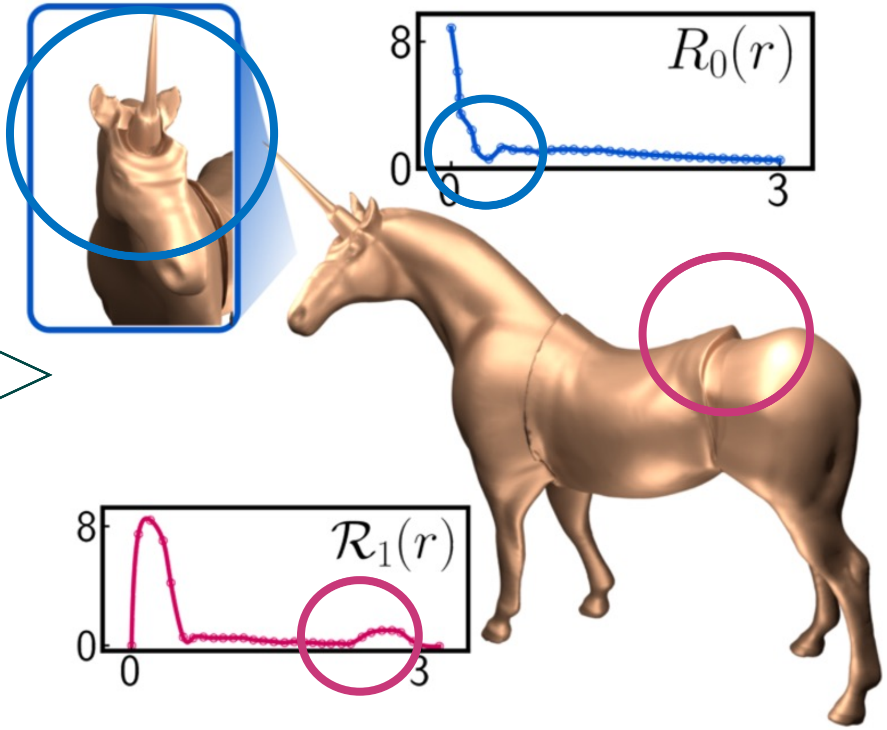

# CONSTRAINED DEFORMATION

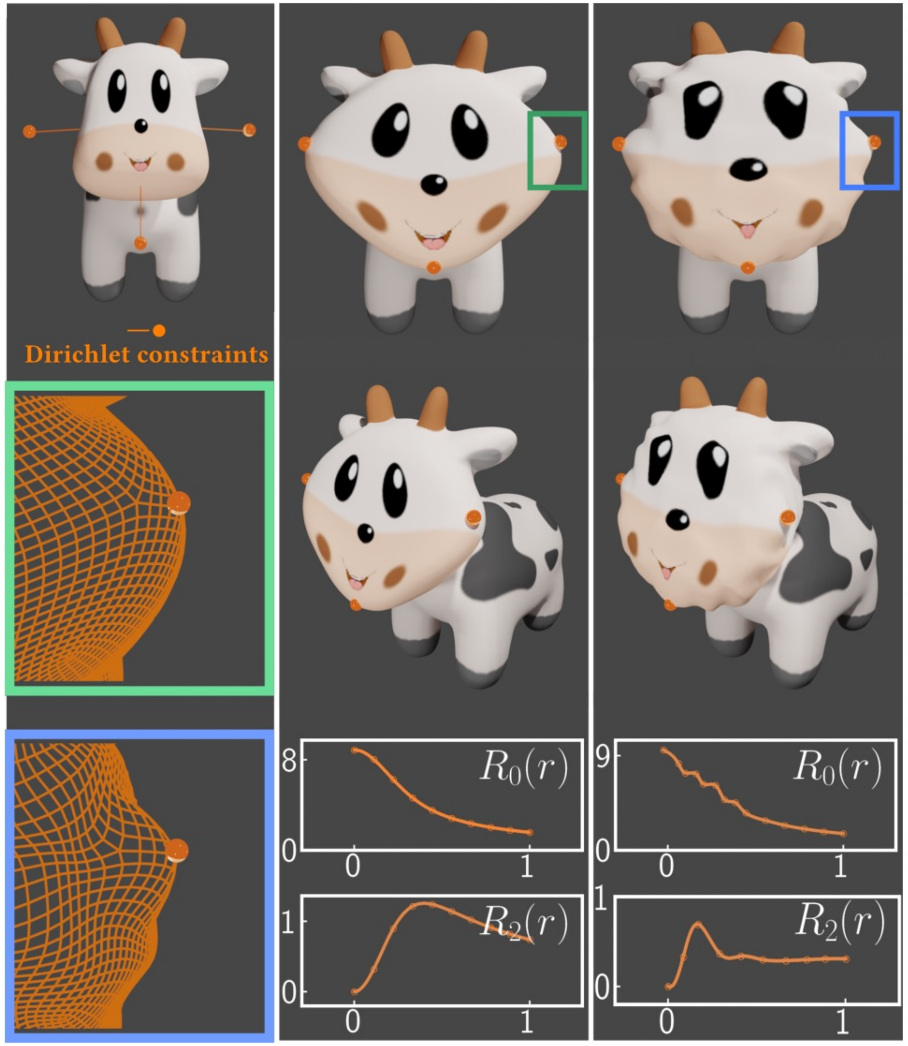


- Solve a dense linear system

$$\begin{bmatrix} \mathrm{Re}[\mathbf{G}(\mathbf{x}_0 - \mathbf{x}_0)] & \dots & \mathrm{Re}[\mathbf{G}(\mathbf{x}_0 - \mathbf{x}_{k-1})] \\ \vdots & \ddots & \vdots \\ \mathrm{Re}[\mathbf{G}(\mathbf{x}_{k-1} - \mathbf{x}_0)] & \dots & \mathrm{Re}[\mathbf{G}(\mathbf{x}_{k-1} - \mathbf{x}_{k-1})] \end{bmatrix} \begin{bmatrix} \mathbf{h}_0 \\ \vdots \\ \mathbf{h}_{k-1} \end{bmatrix} = \begin{bmatrix} \mathbf{u}_0 \\ \vdots \\ \mathbf{u}_{k-1} \end{bmatrix}$$

# SCALABLE INVERSE FACTORIZED PRECONDITIONERS

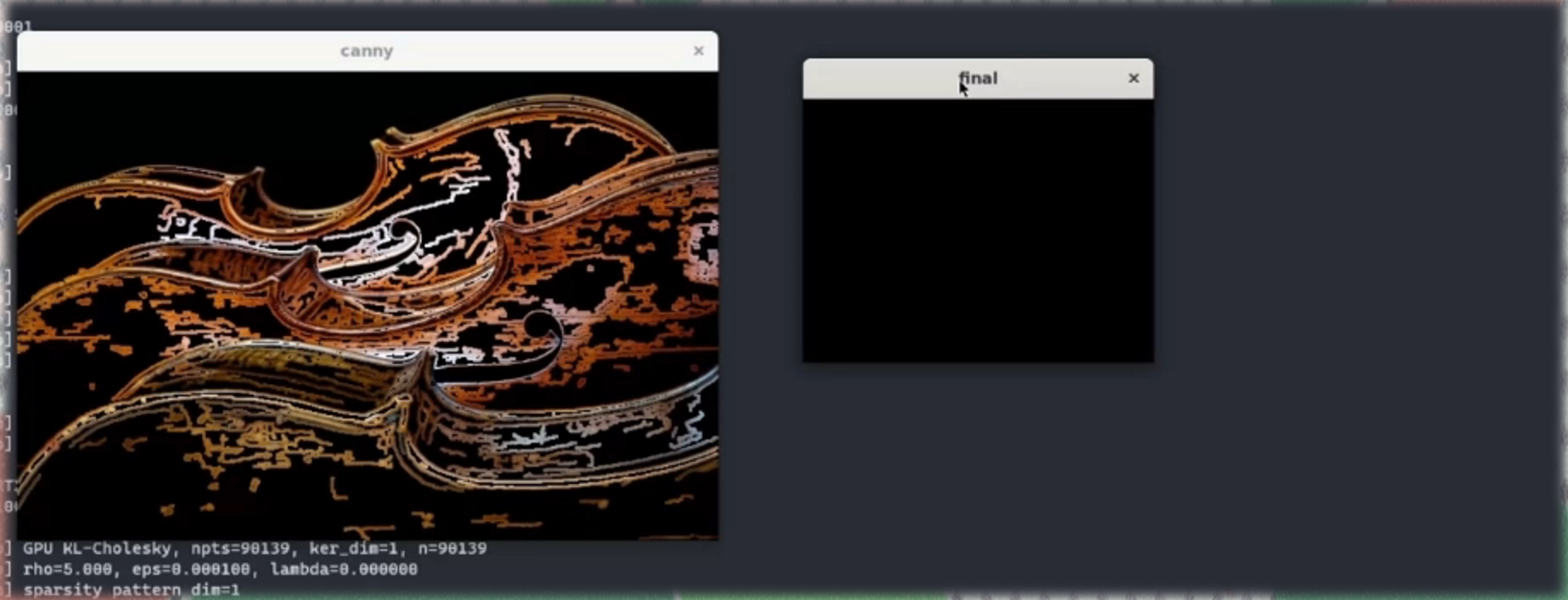

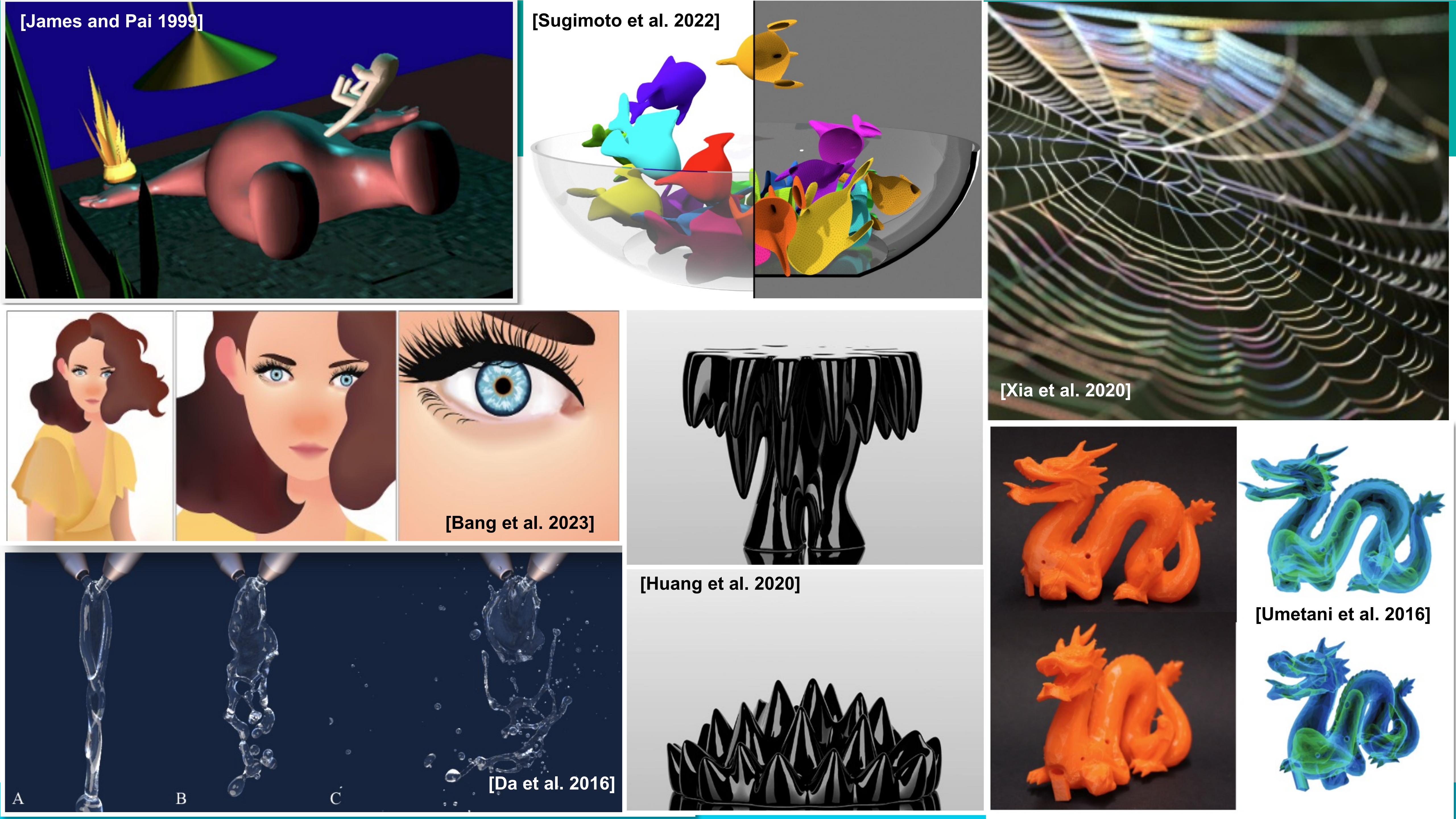
[James and Pai 1999]
[Sugimoto et al. 2022]
[Xia et al. 2020]
[Bang et al. 2023]
[Huang et al. 2020]
[Umetani et al. 2016]
A
B
C
[Da et al. 2016]

# RECAP BEM

- Boundary Element Method (BEM)
  - Turn volumetric differential equations into **boundary integral equations (BIE)**
  - No need for volumetric tessellation, slower growth of the problem size
  - Works for infinite large domains

- Two stages of BEM
  - **SOLVE** for **unknown** boundary data from **given** boundary conditions
    - E.g., boundary charges producing an electric potential field

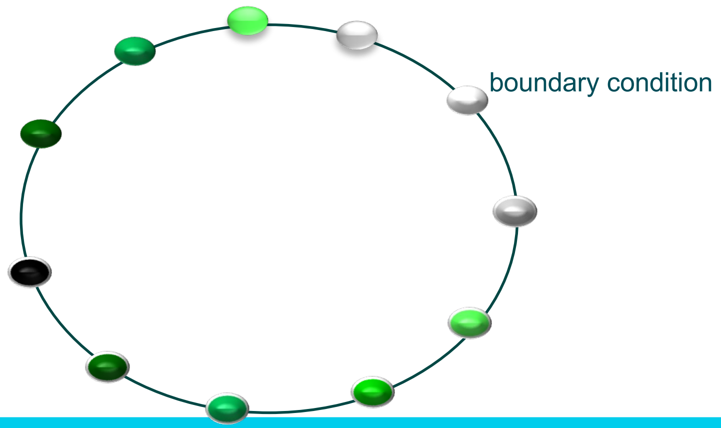


# RECAP BEM

- Boundary Element Method (BEM)
  - Turn volumetric differential equations into **boundary integral equations (BIE)**
  - No need for volumetric tessellation, slower growth of the problem size
  - Works for infinite large domains

- Two stages of BEM
  - **SOLVE** for **unknown** boundary data from **given** boundary conditions
    - E.g., boundary charges producing an electric potential field
  - **EXTRAPOLATE** the solution at arbitrary target points from boundary data

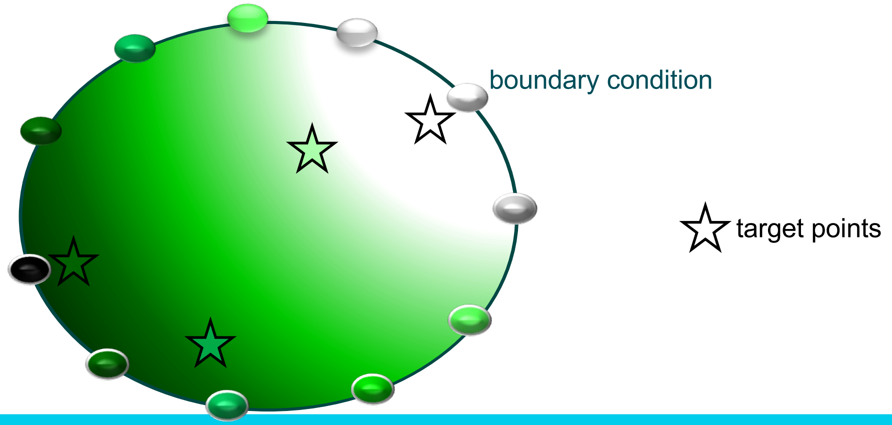


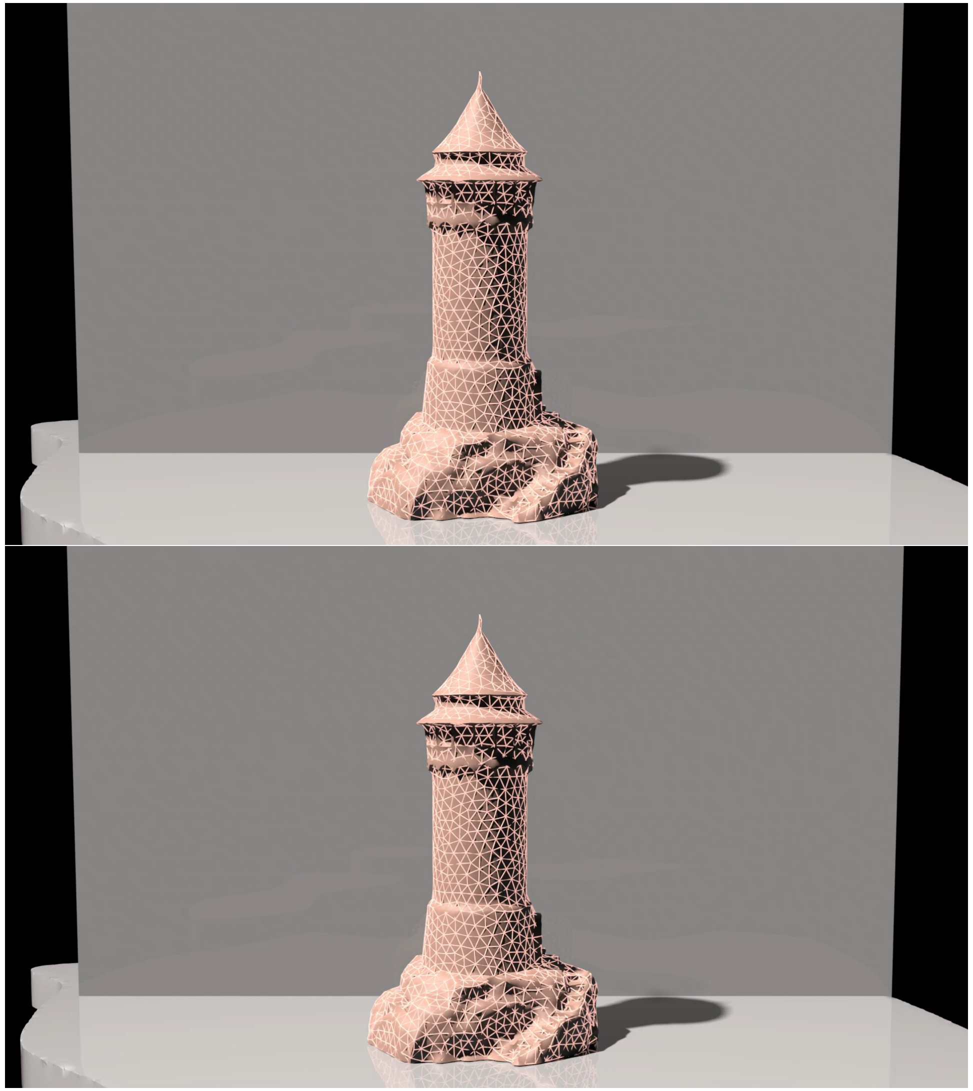

# BOTTLENECK: FINDING BOUNDARY DATA

**PDE**

$$\mathbf{x} \in \Omega, \;\; \Delta u = 0$$

**Representation of the solution**

$$\mathbf{x} \in \mathbb{R}^d \backslash \Gamma, \;\; u(\mathbf{x}) = \underbrace{\int_\Gamma \frac{\partial G(\mathbf{x}, \mathbf{y})}{\partial \mathbf{n}_\mathbf{y}} \sigma(\mathbf{y}) \, \mathrm{d}A_\mathbf{y}}_{\text{Double-layer potential}} - \underbrace{\int_\Gamma G(\mathbf{x}, \mathbf{y}) \tau(\mathbf{y}) \, \mathrm{d}A_\mathbf{y}}_{\text{Single-layer potential}}$$

**BIE**

$$\mathbf{x} \in \Gamma, \; u(\mathbf{x}) = b(\mathbf{x}) \text{ or } \partial_\mathbf{n} u(\mathbf{x}) = g(\mathbf{x})$$

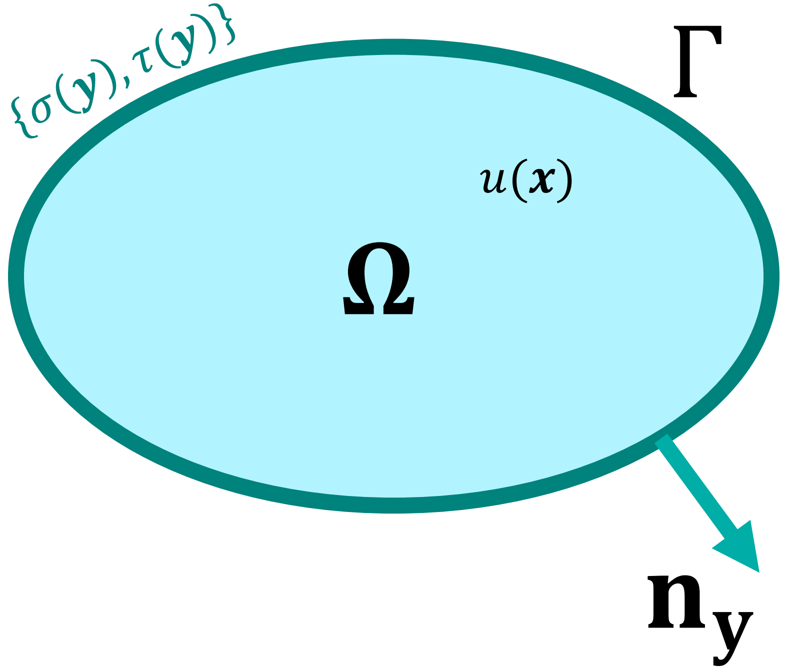

# BOTTLENECK: FINDING BOUNDARY DATA

**PDE**

$$\mathbf{x} \in \Omega, \quad \Delta u = 0$$

**Representation of the solution**

$$\mathbf{x} \in \mathbb{R}^d \backslash \Gamma, \; u(\mathbf{x}) = \underbrace{\int_\Gamma \frac{\partial G(\mathbf{x},\mathbf{y})}{\partial \mathbf{n}_\mathbf{y}} \sigma(\mathbf{y})\, \mathrm{d}A_\mathbf{y}}_{\text{Double-layer potential}} - \underbrace{\int_\Gamma G(\mathbf{x},\mathbf{y}) \tau(\mathbf{y})\, \mathrm{d}A_\mathbf{y}}_{\text{Single-layer potential}}$$

**BIE**

$$\mathbf{x} \in \Gamma, \; u(\mathbf{x}) = b(\mathbf{x}) \text{ or } \partial_\mathbf{n} u(\mathbf{x}) = g(\mathbf{x})$$

$$[u(\mathbf{x})]_\Gamma = 0$$

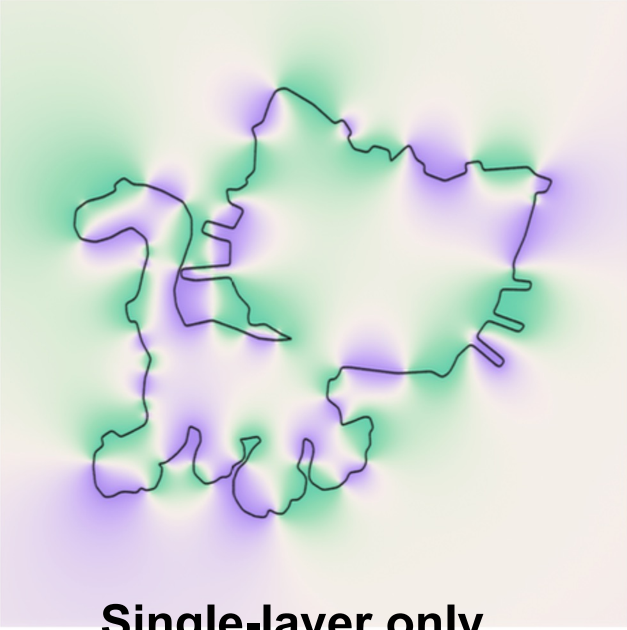

**Single-layer only**

$$[u(\mathbf{x})]_\Gamma = \sigma(\mathbf{x})$$

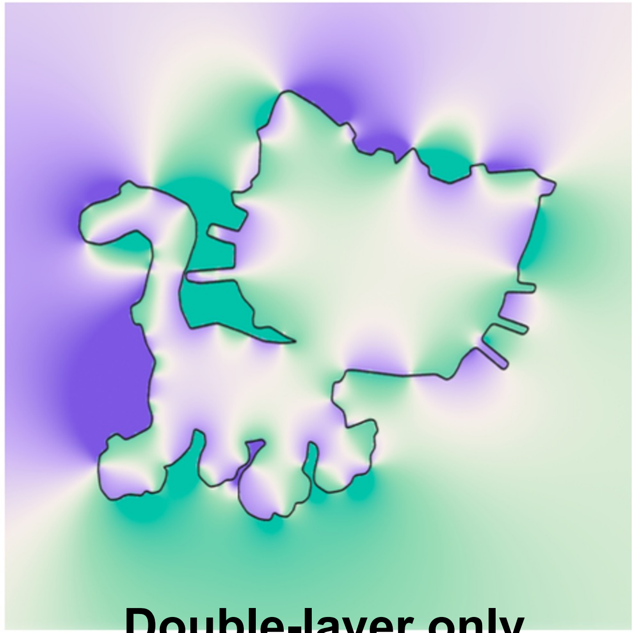

**Double-layer only**

$$u(\mathbf{x})|_{\mathbf{x} \in \mathbb{R}^d \backslash \Omega} = 0$$

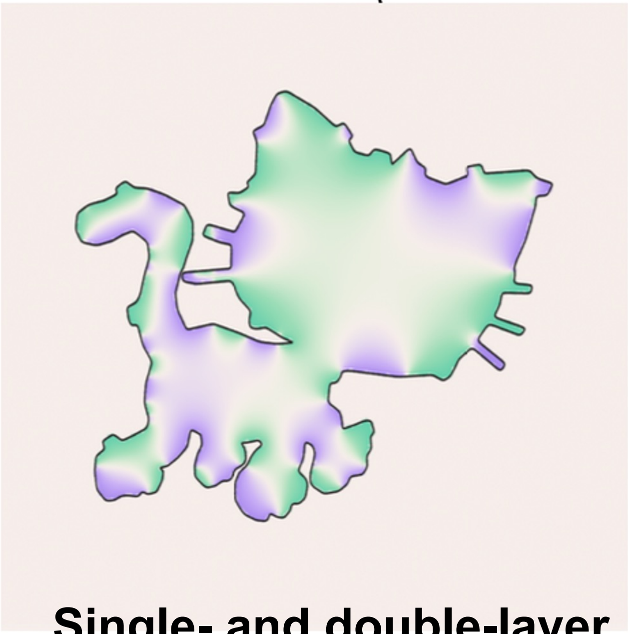

**Single- and double-layer**

# NUMERICAL CHALLENGES POSED BY GREEN'S FUNCTIONS

**BIE**

$\mathbf{x} \in \Gamma,\ u(\mathbf{x}) = b(\mathbf{x})$ or $\partial_{\mathbf{n}} u(\mathbf{x}) = g(\mathbf{x})$

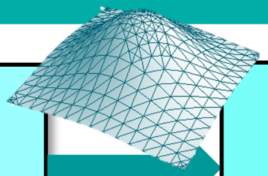

**Linear system**

$$\boldsymbol{Ks = b}$$

**Main culprit:**
**smoothness of the Green's function**

- **The linear system is always dense**
  - Green's functions have non-zero values everywhere
  - Storing the entire system matrix is impossible for big problems
    - **70G** for 100k boundary samples; assembly time is large too!
  - Direct solvers have cubic complexity
- **The linear system is often ill-conditioned***
  - High-frequency vibrations in $\sigma$ get smoothed out after integration
    - So very different $\sigma$'s map to similar $b$, meaning that the BIE is almost degenerate
  - Iterative solvers often struggle to converge
    - multigrid approaches too memory hungry, H-matrices too inaccurate

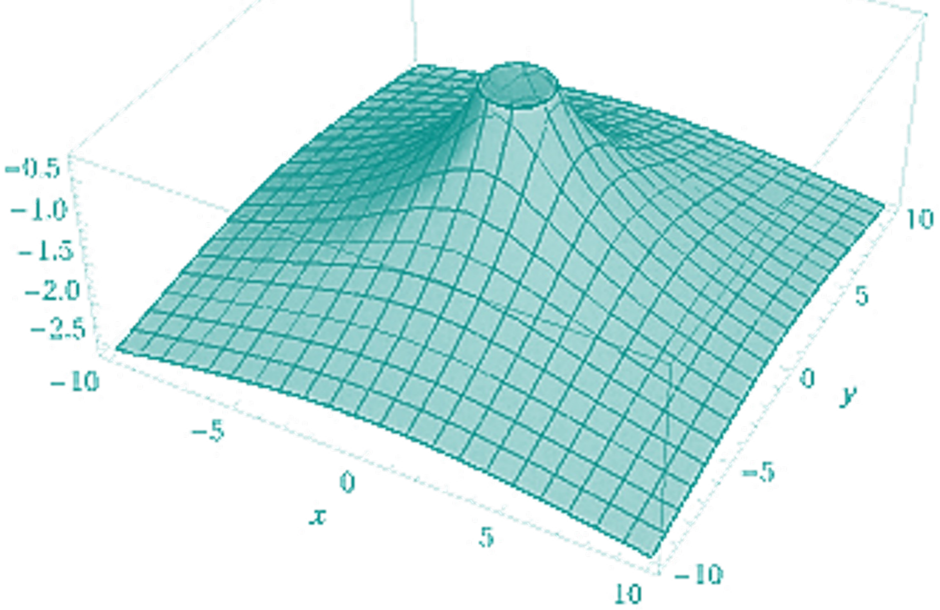


*Fredholm integral equation of the first kind*

$$\mathbf{x} \in \Gamma,\ \int_{\Gamma} G(\mathbf{x},\mathbf{y})\sigma(\mathbf{y})\,\mathrm{d}A_{\mathbf{y}} = b(\mathbf{x})$$

In practice, BIE of ~25K unknowns in recent graphics papers…

## There has to be a better way…

# WHERE SPARSITY EMERGES

- Boundary integral operators are conceptually close to the **inverse** of their differential operator
  - Green function is the solution subject to a singular impulse
  - E.g., in elasticity, a BIE matrix acts like the inverse of stiffness, or compliance
- So, the inverse of BIE matrices could be sparse
  - True for many covariance matrices assembled by fast-decaying kernel functions in Gaussian Process
  - Similar for Green's functions as well

Compliance Displacements

$$Ks = b$$

Forces

[Chow and Saad 2014]

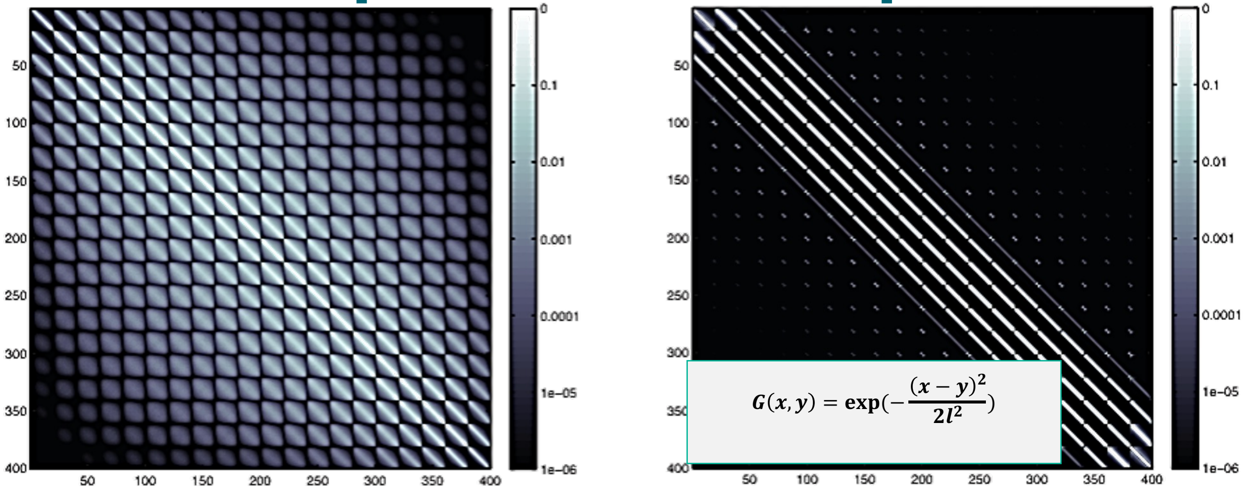


(a) Inverse Laplacian matrix (b) Inverse exponential covariance matrix

# SYMMETRIC CASE: INVERSE CHOLESKY FACTORIZATION

- [Chen et al. 2024] computed inverse Cholesky factors to accelerate PCG

$$Ks = b \Rightarrow K^{-1} \approx L_S L_S^T \Rightarrow s \approx L_S L_S^T b$$

- Kaporin's construction for $L_S$ [Kaporin 1994]

$$L_{S_j,j} = \frac{K^{-1}_{S_j,S_j} e_j}{\sqrt{e_j^{\mathsf{T}} K^{-1}_{S_j,S_j} e_j}}, \quad \forall j = 1..B,$$

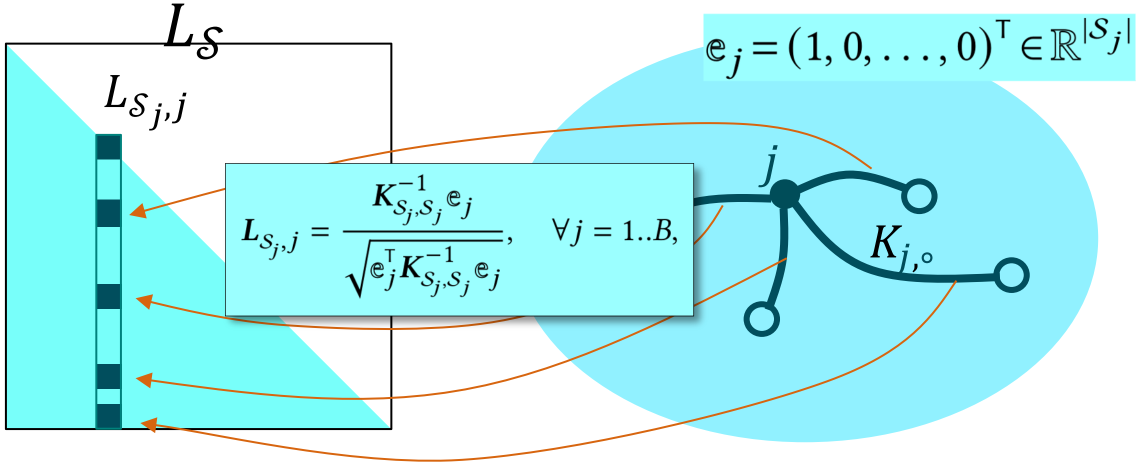


- Properties
  - **Massively parallel:** each column of $L_S$ is computed independently of others. Perfect for GPUs!
  - **Memory efficient:** no need to assemble the global BIE matrix.
  - **Stable:** no breakdowns will occur
  - **Variational interpretation(s):** minimizing Kaporin's condition number*, KL-divergence, and a constrained quadratic form

$^*\ \kappa_{\text{Kap}}(M) = \frac{1}{B} \frac{\operatorname{tr}(M)}{\det(M)^{1/B}}$

# HANDLING NON-SYMMETRIC CASES

SCA 2025

## Dirichlet boundary condition

$$\forall \mathbf{x} \in \Gamma, \quad \int_{\Gamma} G(\mathbf{x}, \mathbf{y}) \sigma(\mathbf{y}) \, dA_{\mathbf{y}} = b(\mathbf{x})$$

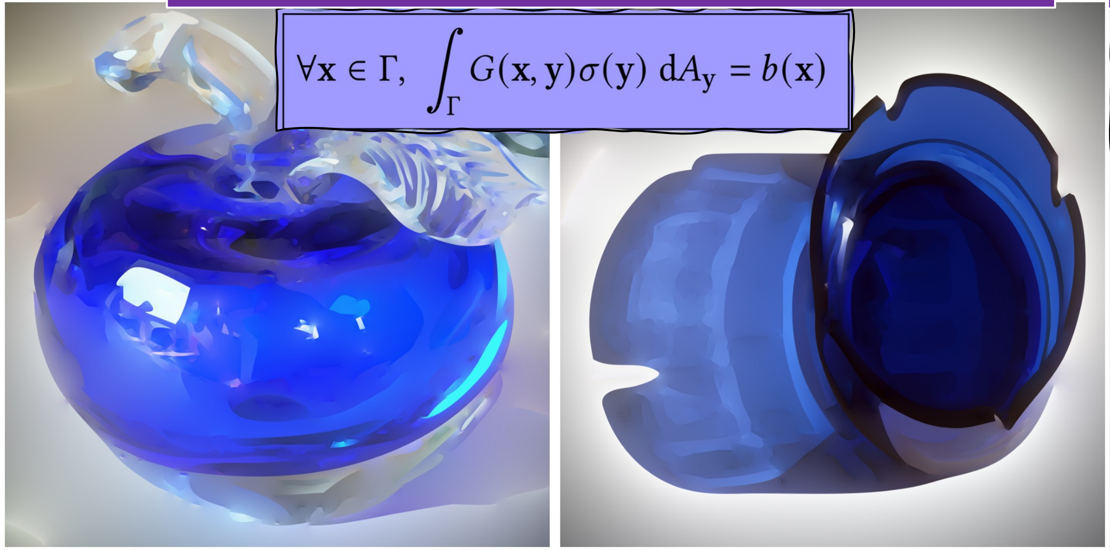

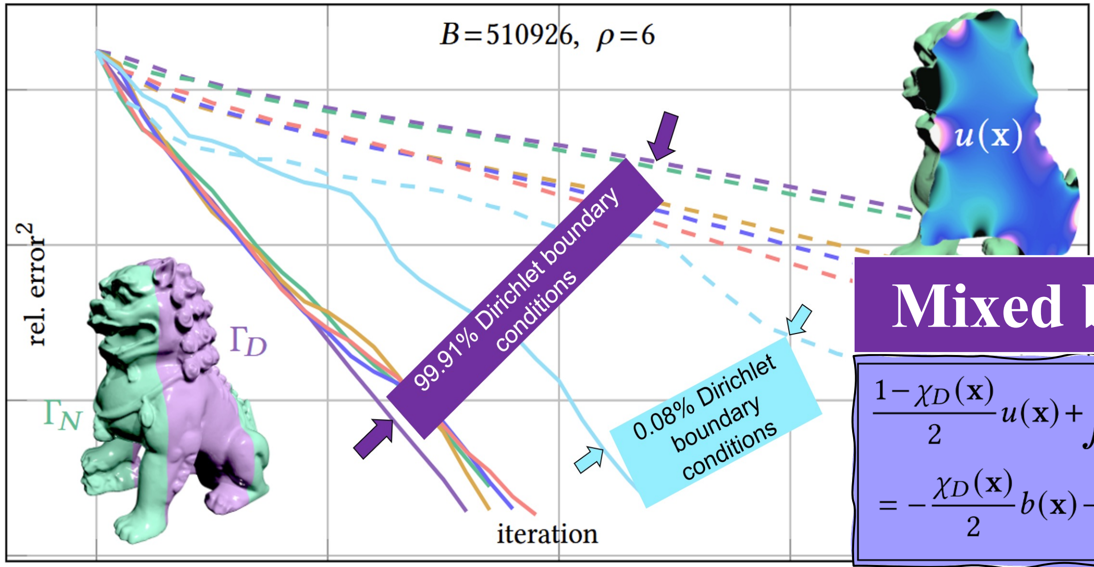


## Neumann boundary condition

$$\forall \mathbf{x} \in \Gamma, \quad \frac{2 + \chi}{2\chi} \sigma(\mathbf{x}) + \int_{\Gamma} \frac{\partial G(\mathbf{x}, \mathbf{y})}{\partial \mathbf{n}_{\mathbf{x}}} \sigma(\mathbf{y}) \, dA_{\mathbf{y}} = \mathbf{H}_{\text{ext}} \cdot \mathbf{n}$$

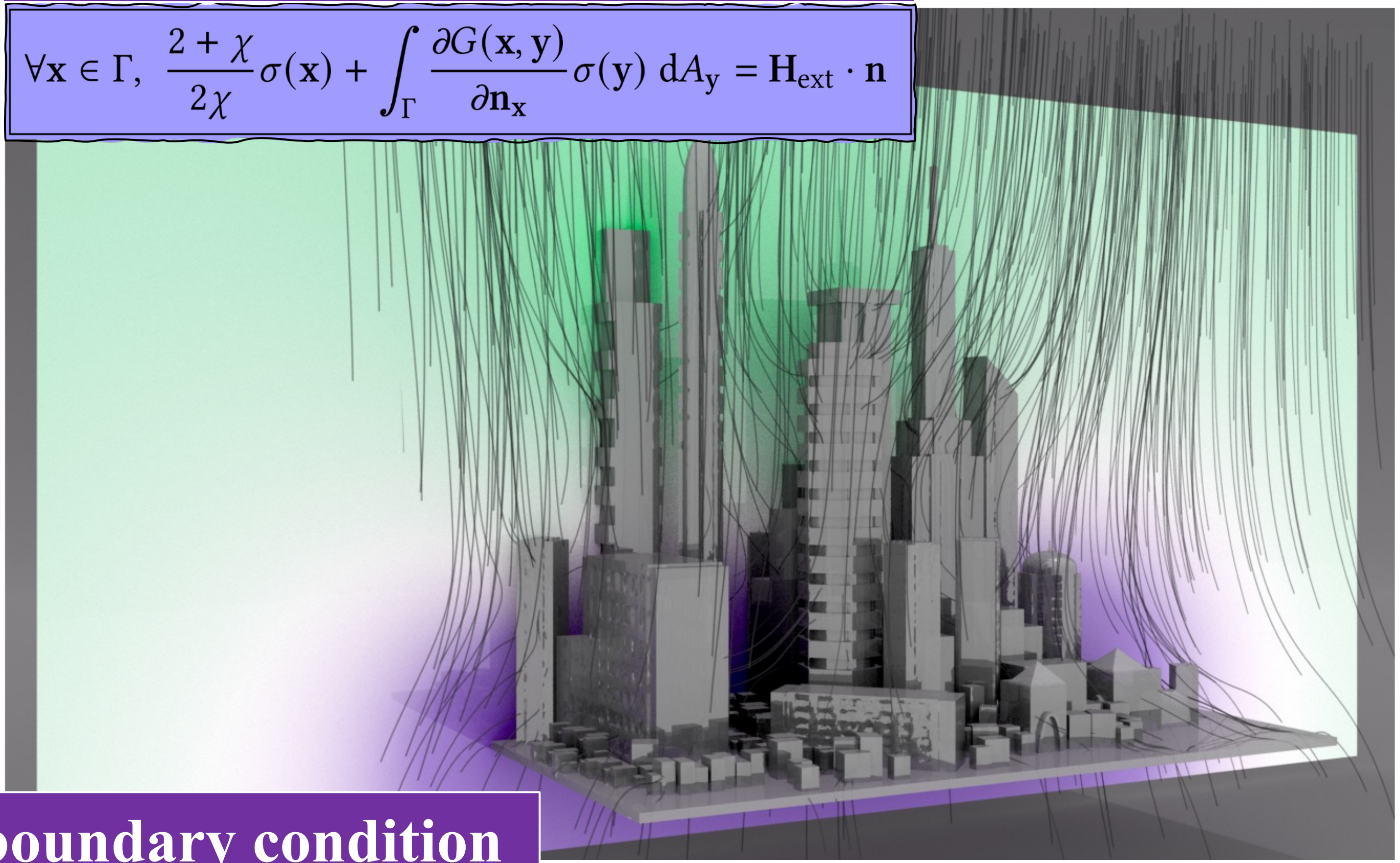

## Mixed boundary condition

$$\frac{1 - \chi_D(\mathbf{x})}{2} u(\mathbf{x}) + \int_{\Gamma_N} \frac{\partial G(\mathbf{x}, \mathbf{y})}{\partial \mathbf{n}_{\mathbf{y}}} u(\mathbf{y}) dA_{\mathbf{y}} - \int_{\Gamma_D} G(\mathbf{x}, \mathbf{y}) \frac{\partial u(\mathbf{y})}{\partial \mathbf{n}_{\mathbf{y}}} dA_{\mathbf{y}}$$
$$= -\frac{\chi_D(\mathbf{x})}{2} b(\mathbf{x}) - \int_{\Gamma_D} \frac{\partial G(\mathbf{x}, \mathbf{y})}{\partial \mathbf{n}_{\mathbf{y}}} b(\mathbf{y}) dA_{\mathbf{y}} + \int_{\Gamma_N} G(\mathbf{x}, \mathbf{y}) g(\mathbf{y}) dA_{\mathbf{y}}$$

# REORDERING & SPARSITY PATTERN

## REORDERING

- Goal: **evenly** distributing point samples
  - Farthest point sampling, i.e., coarse-to-fine

$$i_k = \underset{q}{\operatorname{argmax}} \min_{p\in\{0,k-1\}} \operatorname{dist}(\boldsymbol{y}_q, \boldsymbol{y}_{i_p}),$$

  - Reverse it $\boldsymbol{P} = \{i_{B-1}, \ldots, i_1, i_0\}$, i.e., fine-to-coarse

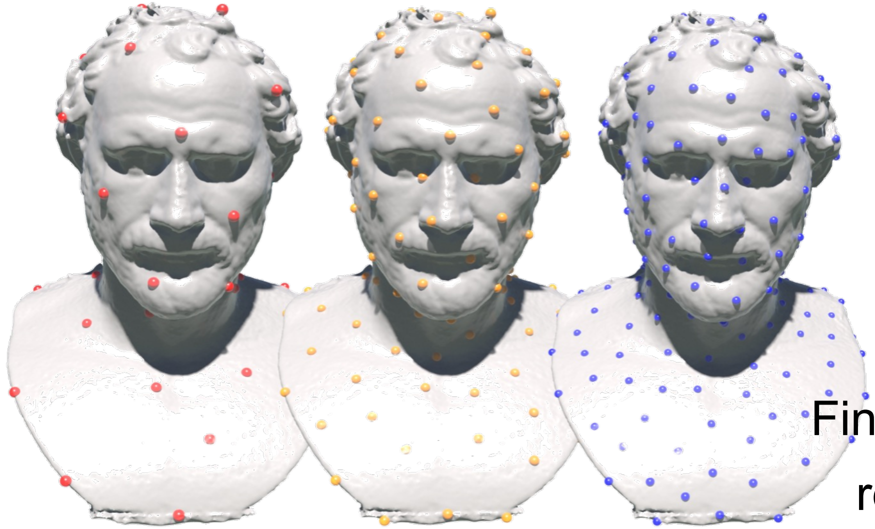

last 50 last 150 last 250

Fine-to-coarse reordering

## SPARSITY PATTERN

- Capturing those **"important"** nonzero fill-ins
  - Length scale returned in coarse-to-fine ordering

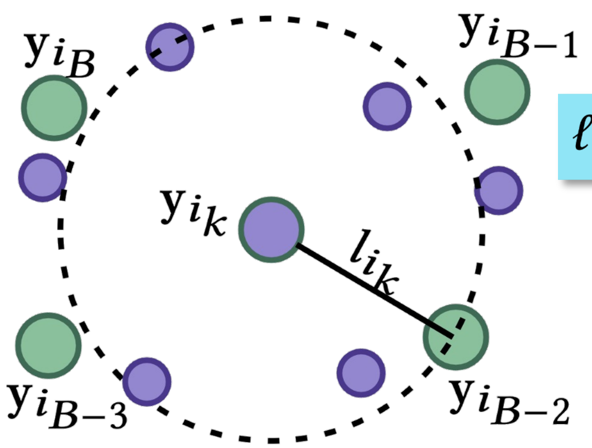


$$\ell_{i_k} = \min_{p\in\{0,k-1\}} \operatorname{dist}(\boldsymbol{y}_{i_k}, \boldsymbol{y}_{i_p})$$

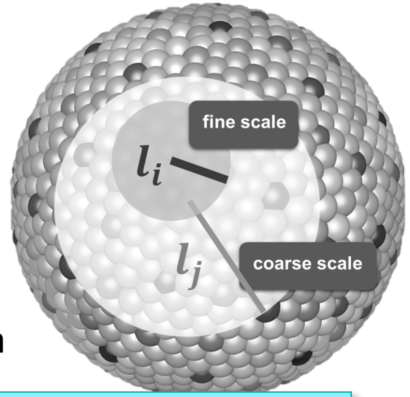


  - Lower-triangular, multiscale sparsity pattern

$$S := \{(i, j) | i \geq j \text{ and } \operatorname{dist}(x_i, x_j) \leq \rho \min(\ell_i, \ell_j)\}$$

# SCREENING EFFECT



- Observed in Gaussian process based regression [Stein 2002]
  - E.g., Matern covariance function
- Probabilistic interpretation
  - Green's function is smooth, impliying long-range correlations between points
  - Conditioning a smooth process on values near a target point weakens the target's correlation with more distant points

$$p(A,B,C,D) = p(A)p(B|A)p(C|A,B)p(D|A,B,C) = N(0,\Sigma)$$

$$p(A,B,C,D) \approx p(A)p(B|A)p(C|A,\cancel{B})p(D|A,B,\cancel{C}) = N(0,(LL^{\mathrm{T}})^{-1})$$

Too far      Too far

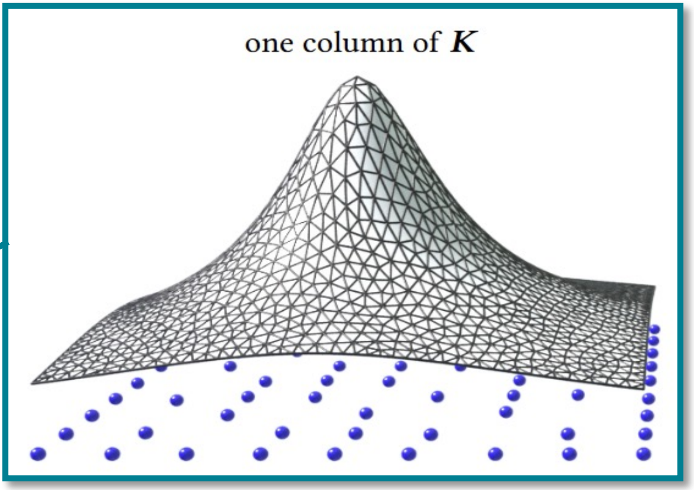


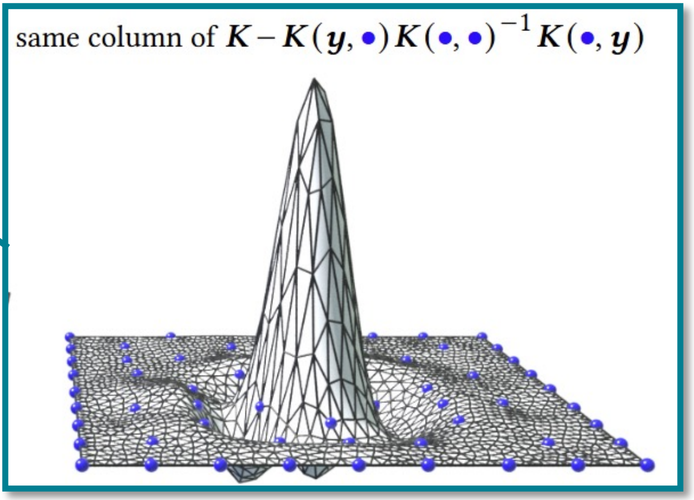

# PROOF OF CONCEPT

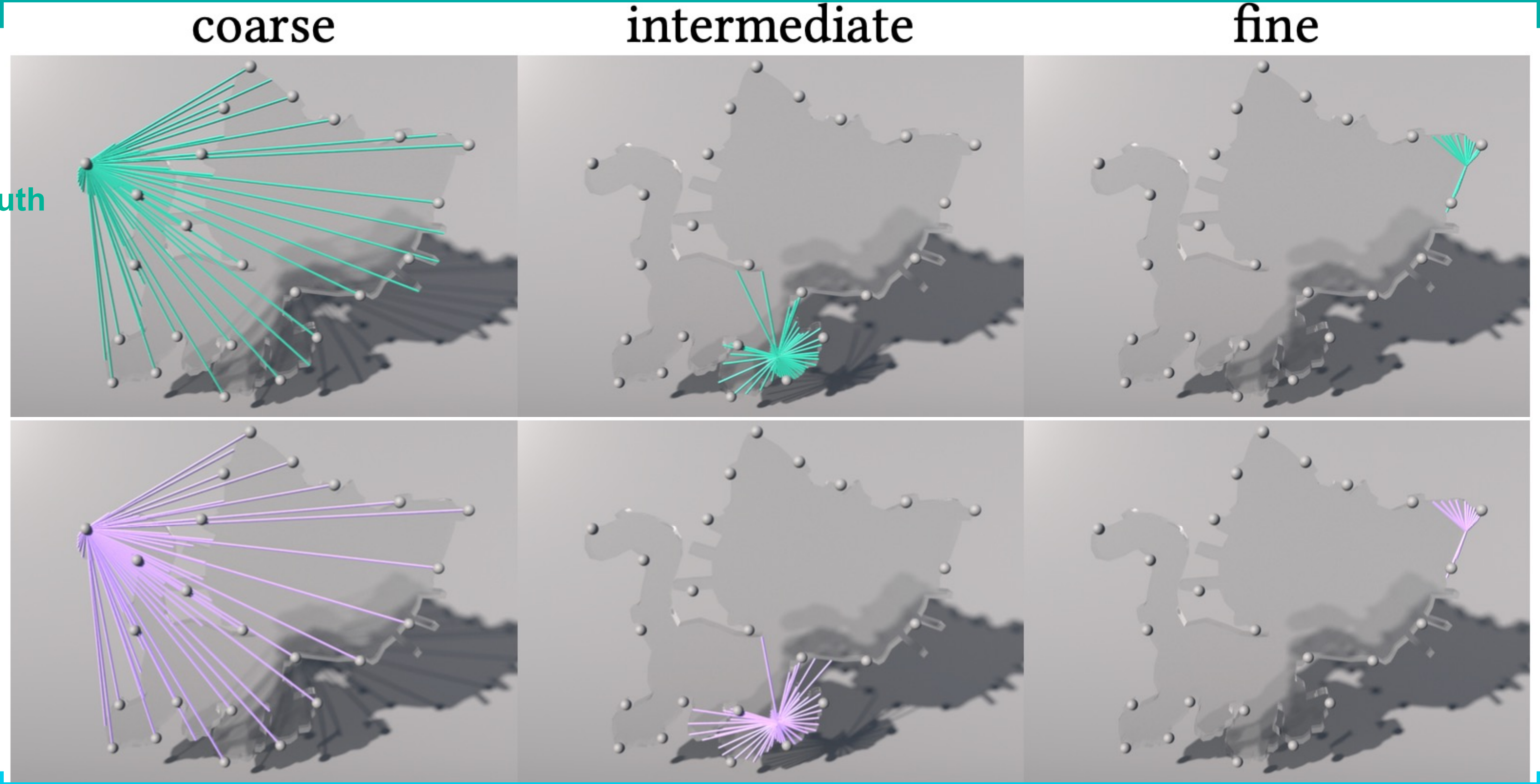


Ground-truth pattern

Max-min pattern

# AN INTERESTING PARADOX

- Smoothness of the Green's function responsible for all the numerical challenges
- … but also key to solve these problems
  - because the information provided by nearby points renders that of distant points redundant
  - proper reordering disentangles the complex correlations between points

# EXAMPLES OF APPLICATION

SCA2025

Laplace's equation

$$\Delta u = 0$$

$$G(\boldsymbol{x},\boldsymbol{y}) = \begin{cases} -\frac{1}{2\pi}\ln(r), & \text{in 2D} \\ \frac{1}{4\pi r}, & \text{in 3D} \end{cases}$$

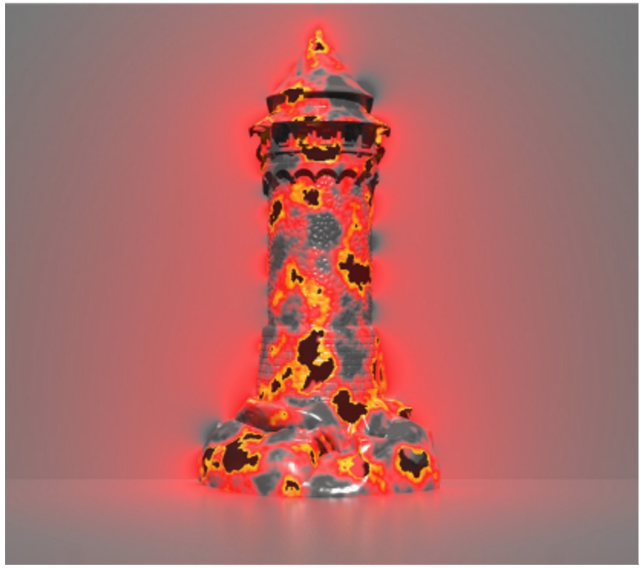

Linear elasticity

$$\Delta u + \frac{1}{1-2\nu}\nabla(\nabla\cdot u) = 0,$$

$$G(\boldsymbol{x},\boldsymbol{y}) = \begin{cases} \frac{a-b}{r}\ln(1/r)\boldsymbol{I} + \frac{b}{r^2}\boldsymbol{r}\boldsymbol{r}^{\mathsf{T}}, & \text{in 2D} \\ \frac{a-b}{r}\boldsymbol{I} + \frac{b}{r^3}\boldsymbol{r}\boldsymbol{r}^{\mathsf{T}}, & \text{in 3D} \end{cases}$$

Helmholtz equation

$$\Delta u + k^2 u = 0,$$

$$G(\boldsymbol{x},\boldsymbol{y}) = \begin{cases} \frac{\mathbb{i}}{4}H_0^{(1)}(kr), & \text{in 2D,} \\ \frac{\exp(\mathbb{i}kr)}{4\pi r}, & \text{in 3D,} \end{cases}$$

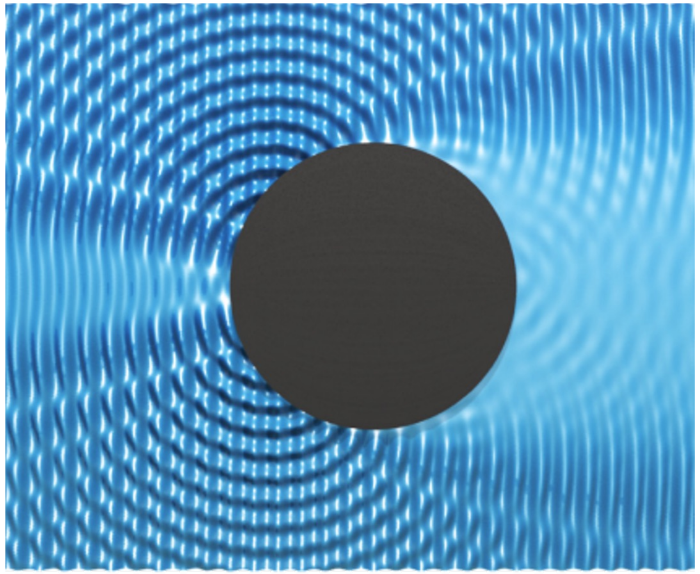

# LAPLACE'S EQUATION

# LAPLACE’S EQUATION

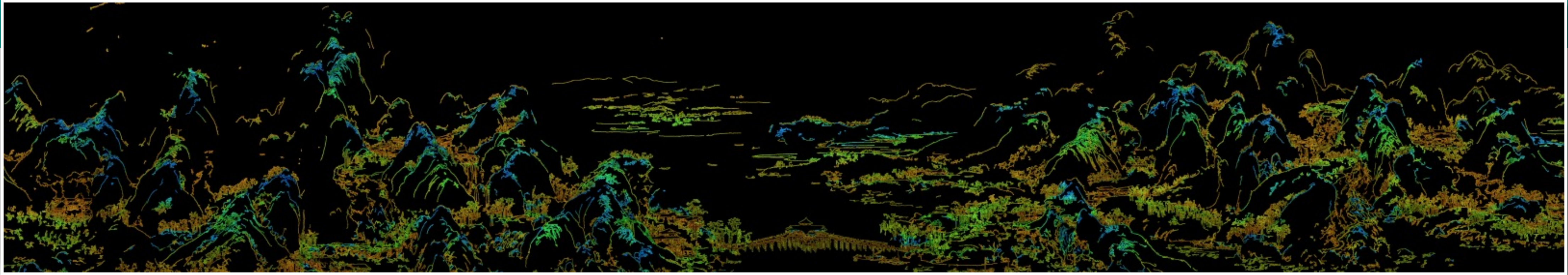

# LAPLACE'S EQUATION

SCA 2025

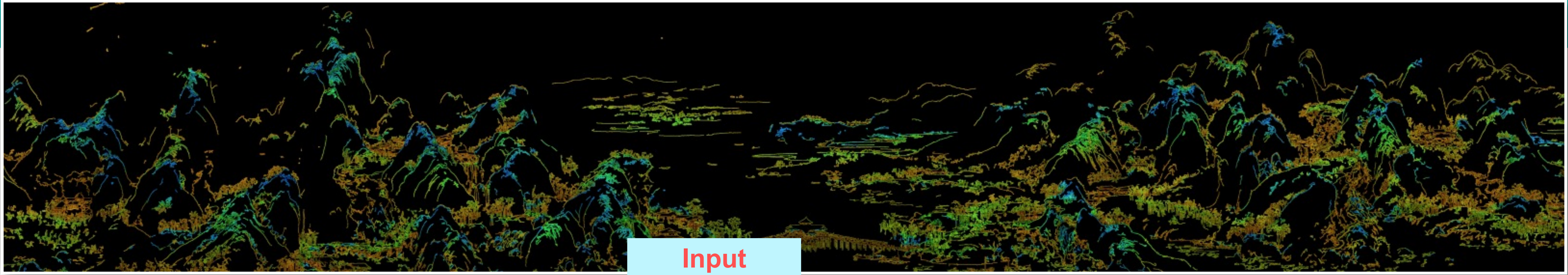

Input

#DoF > 1M

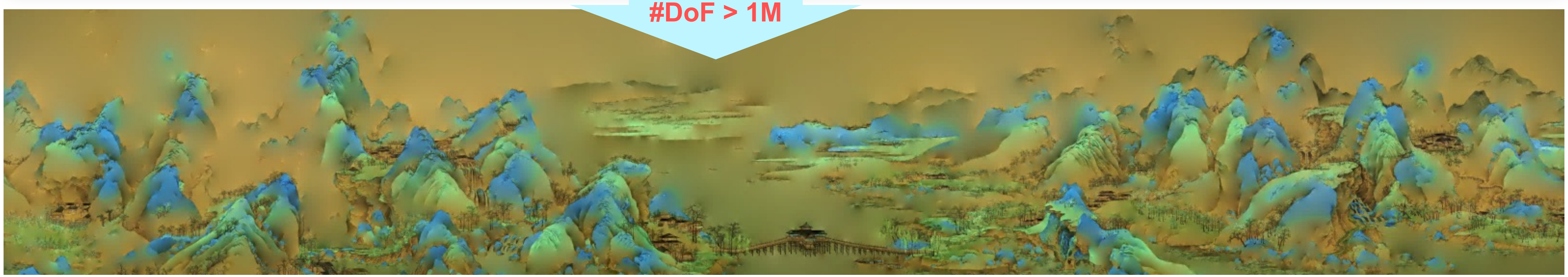

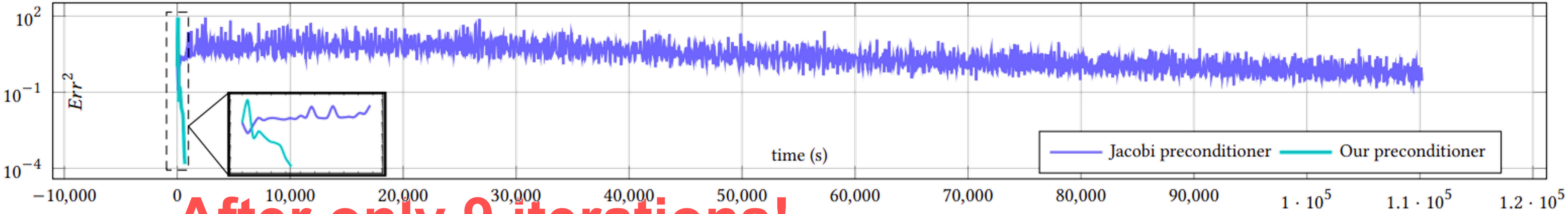


**After only 9 iterations!**

# LINEAR ELASTICITY


**Constrained Kelvinlet deformer** [de Goes and James 2017]

# HELMHOLTZ EQUATION

# boundary points=12.7K

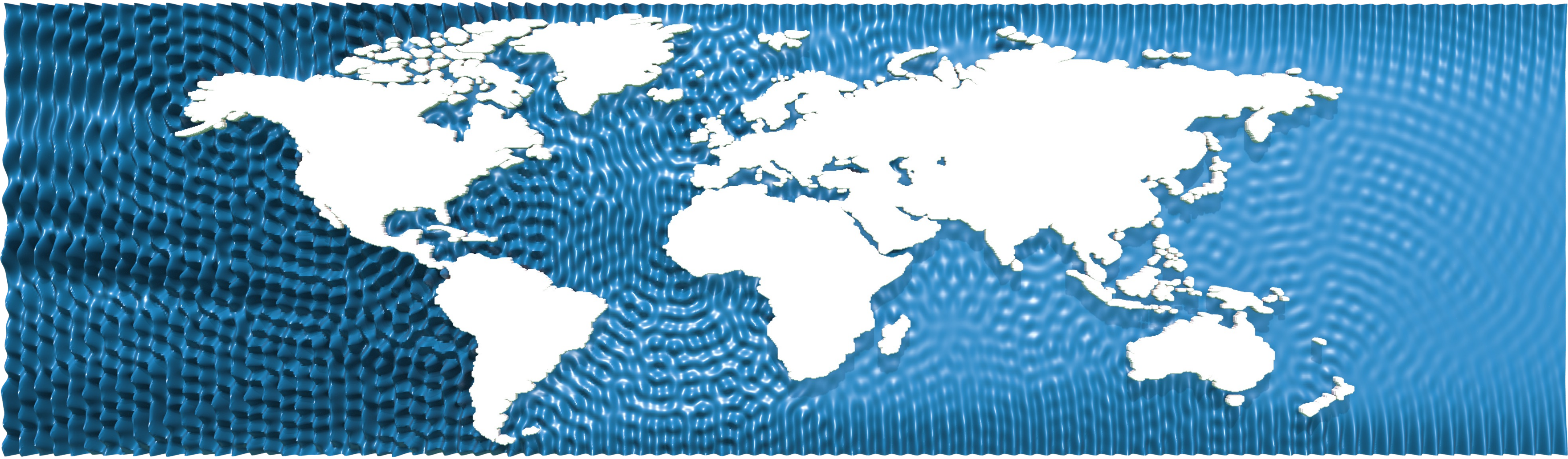

# BEM FROM GAUSSIAN PROCESS VIEWPOINT

- Formulate stochasticity in Computer Graphics
  - Geometry processing, e.g., surface reconstruction [Sellán and Jacobson 2022]
  - Rendering, e.g., light transport [Seyb et al. 2024]
- Boundary value problems from a statistical point of view
  - Investigate the distribution of all possible solutions, not just a single one!
- Gaussian-process based inference *vs.* MFS
  - Beyond conditional mean

$$\mu\left(f(\boldsymbol{x}) \mid \boldsymbol{y}, f(\boldsymbol{y})\right) = \boldsymbol{K}(\boldsymbol{x},\boldsymbol{y})\boldsymbol{K}(\boldsymbol{y},\boldsymbol{y})^{-1} f(\boldsymbol{y}),$$

  - Conditional variance for uncertainty quantification

$$\sigma^2_{\boldsymbol{y}_i} = \boldsymbol{K}(\boldsymbol{y}_i,\boldsymbol{y}_i) - \boldsymbol{K}(\boldsymbol{y}_i,\boldsymbol{x})\boldsymbol{K}(\boldsymbol{x},\boldsymbol{x})^{-1}\boldsymbol{K}(\boldsymbol{x},\boldsymbol{y}_i).$$

  - Tell the probability of the solution falling within a given range

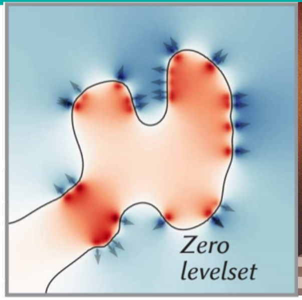


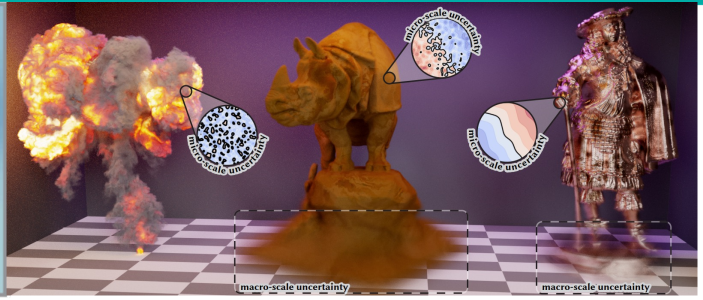


| Gaussian Process | MFS |
|---|---|
| Kernel function | Green's function |
| Observation | Boundary condition |
| Conditional mean | Solution |
| Prediction | Evaluation |

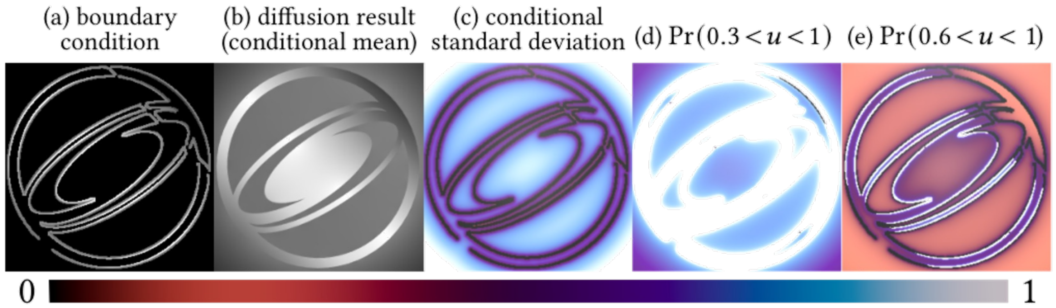


Uncertainty quantification of BIE solves

# GENERALIZED BARYCENTRIC COORDINATES

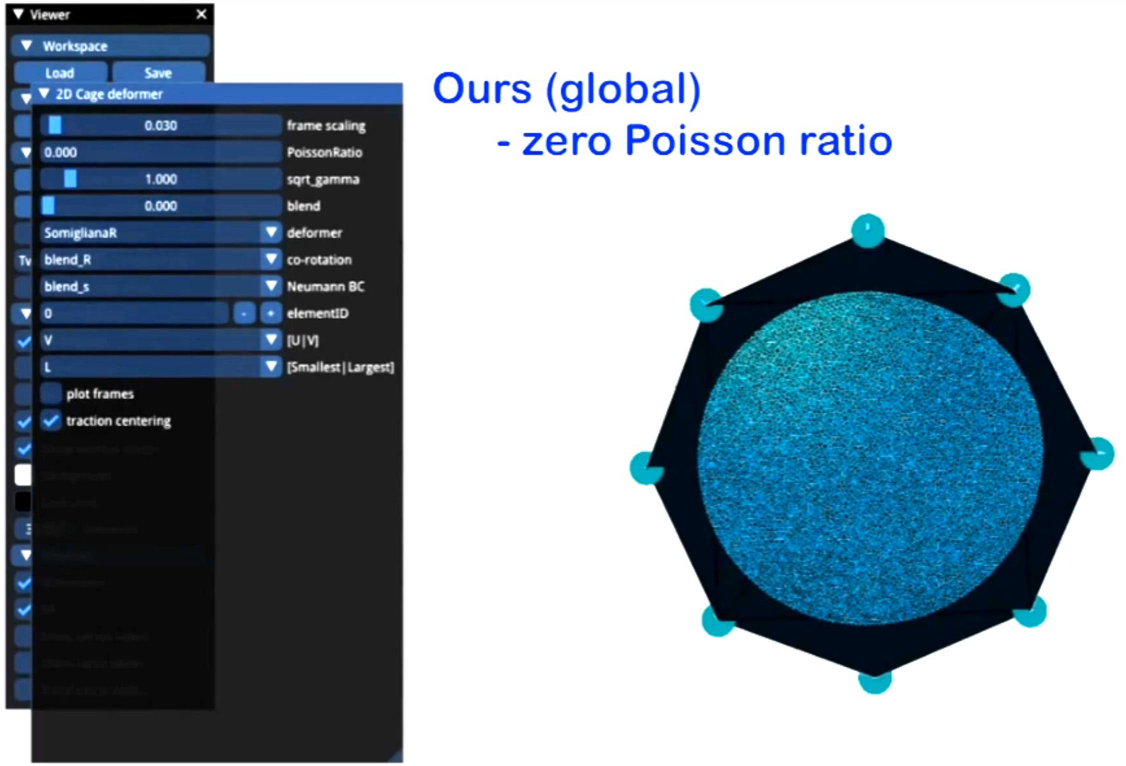

# CAGE DEFORMER

- Cage deformer
  - **Boundary-aware and extremely fast**
  - Based on generalized barycentric coordinates
    - many options available now (see our survey [Ströter et al. 2024])

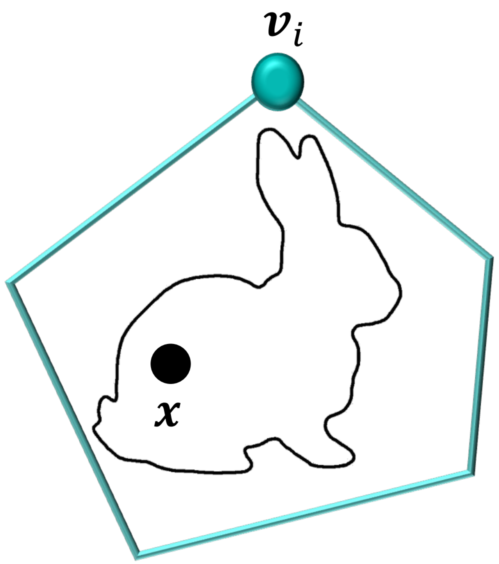


$$\boldsymbol{x} = \sum_i \phi_i(\boldsymbol{x})\boldsymbol{v}_i$$

$$\tilde{\boldsymbol{x}}(\boldsymbol{x}) = \sum_i \phi_i(\boldsymbol{x})\tilde{\boldsymbol{v}}_i$$

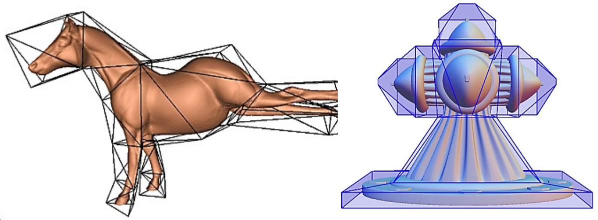

**Mean-value coords** [Floater 2003; Ju et al. 2005; Thiery et al. 2018]

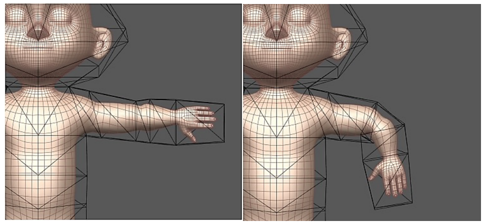

**Harmonic coords** [Joshi et al. 2007]

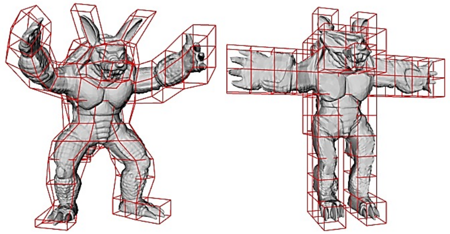

**Maximum entropy coords** [Hormann and Sukumar 2008]

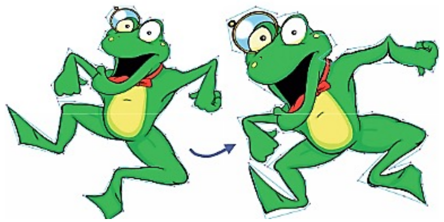

**Complex coords** [Weber et al. 2009]

# CAGE DEFORMER

- Cage deformer
  - **Boundary-aware and extremely fast**
  - Based on generalized barycentric coordinates
    - many options available now (see our survey [Ströter et al. 2024])

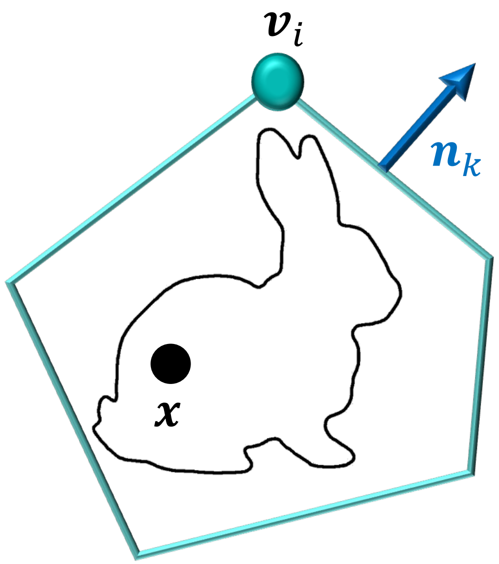


$$\boldsymbol{x} = \sum_i \phi_i(\boldsymbol{x})\boldsymbol{v}_i + \sum_k \psi_k(\boldsymbol{x})\boldsymbol{n}_k$$

$$\tilde{\boldsymbol{x}}(\boldsymbol{x}) = \sum_i \phi_i(\boldsymbol{x})\tilde{\boldsymbol{v}}_i + \sum_k \psi_k(\boldsymbol{x})\,(c_k\tilde{\boldsymbol{n}}_k)$$

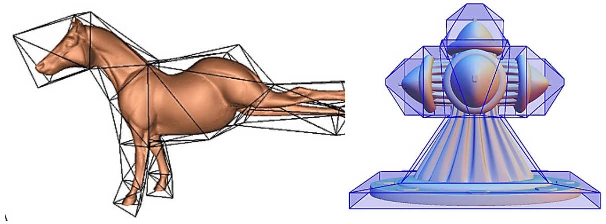

**Mean-value coords** [Floater 2003; Ju et al. 2005; Thiery et al. 2018]

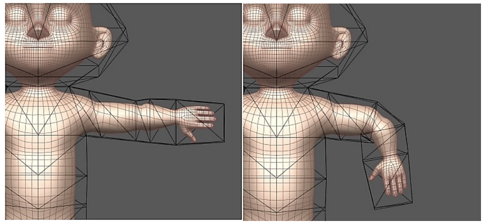

**Harmonic coords** [Joshi et al. 2007]

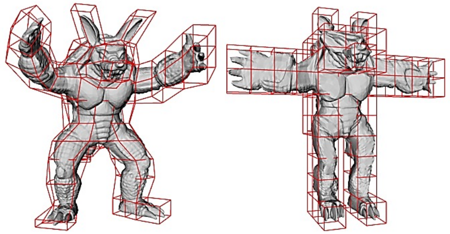

**Maximum entropy coords** [Hormann and Sukumar 2008]

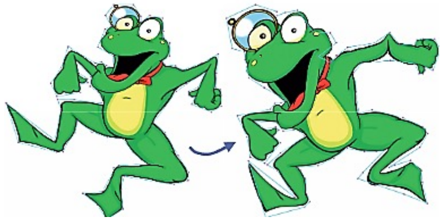

**Complex coords** [Weber et al. 2009]

**+ Green coordinates** [Lipman et al. 2008]

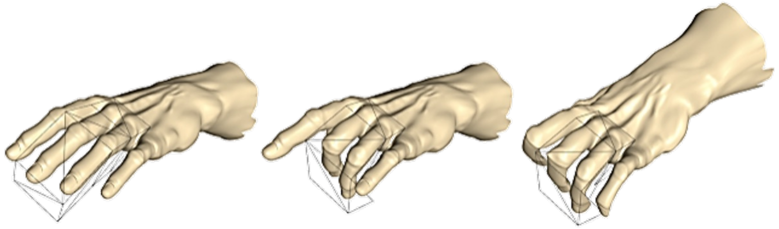

# GENERALIZED BARYCENTRIC COORDINATES WITH NORMAL CONTROL

| | Green coordinates [Lipman et al. 2008] | Somigliana coordinates [Chen et al. 2023] | Biharmonic coordinates [Thiery et al. 2024] |
|---|---|---|---|
| **PDE** | $\Delta \boldsymbol{u} = \boldsymbol{0}$ | $\Delta \boldsymbol{u} + \frac{1}{1-2\nu}\nabla(\nabla \cdot \boldsymbol{u}) = \boldsymbol{0}$ | $\Delta^2 \boldsymbol{u} = \boldsymbol{0}$ |
| **Green's functions** | $G(\boldsymbol{y},\boldsymbol{x}) = \begin{cases} -\frac{1}{4\pi r}, & d=3, \\ \frac{1}{2\pi}\log(r), & d=2. \end{cases}$ | $\mathcal{K}(\boldsymbol{x},\boldsymbol{y}) = \begin{cases} \frac{a-b}{r}\boldsymbol{I} + \frac{b}{r^3}\boldsymbol{r}\boldsymbol{r}^t, & d=3, \\ (b-a)\log(r)\boldsymbol{I} + \frac{b}{r^2}\boldsymbol{r}\boldsymbol{r}^t, & d=2. \end{cases}$ | $\begin{cases} G(\boldsymbol{y},\boldsymbol{x}) = -\frac{1}{4\pi r} \\ \bar{G}(\boldsymbol{y},\boldsymbol{x}) = -\frac{r}{8\pi} \end{cases}$ |
| **Boundary integral reformulation** | $\boldsymbol{u}(\boldsymbol{x}) = \int_{\partial\Omega} [\nabla_{\boldsymbol{n}} G(\boldsymbol{y},\boldsymbol{x})\boldsymbol{u}(\boldsymbol{y}) - G(\boldsymbol{y},\boldsymbol{x})\nabla_{\boldsymbol{n}}\boldsymbol{u}(\boldsymbol{y})]\, \mathrm{d}A_{\boldsymbol{y}}$ | $\boldsymbol{u}(\boldsymbol{x}) = \int_{\partial\Omega} [\mathcal{T}(\boldsymbol{y},\boldsymbol{x})\boldsymbol{u}(\boldsymbol{y}) + \mathcal{K}(\boldsymbol{y},\boldsymbol{x})\boldsymbol{\tau}(\boldsymbol{y})]\, \mathrm{d}A_{\boldsymbol{y}}$ | $\boldsymbol{u}(\boldsymbol{x}) = \int_{\partial\Omega} [\boldsymbol{u}(\boldsymbol{y})\nabla_{\boldsymbol{n}} G(\boldsymbol{y},\boldsymbol{x}) - G(\boldsymbol{y},\boldsymbol{x})\nabla_{\boldsymbol{n}}\boldsymbol{u}(\boldsymbol{y}) + \Delta\boldsymbol{u}(\boldsymbol{y})\nabla_{\boldsymbol{n}}\bar{G}(\boldsymbol{y},\boldsymbol{x}) - \bar{G}(\boldsymbol{y},\boldsymbol{x})\nabla_{\boldsymbol{n}}\Delta\boldsymbol{u}(\boldsymbol{y})]\, \mathrm{d}A_{\boldsymbol{y}}$ |

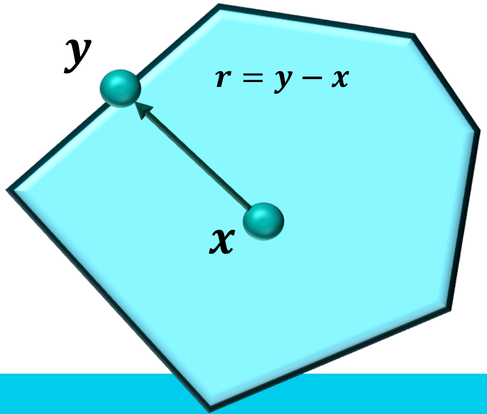

# GENERALIZED BARYCENTRIC COORDINATES WITH NORMAL CONTROL

SCA 2025

| | Green coordinates [Lipman et al. 2008] | Somigliana coordinates [Chen et al. 2023] | Biharmonic coordinates [Thiery et al. 2024] |
|---|---|---|---|
| **PDE** | $\Delta \boldsymbol{u} = \boldsymbol{0}$ | $\Delta \boldsymbol{u} + \frac{1}{1-2\nu}\nabla(\nabla \cdot \boldsymbol{u}) = \boldsymbol{0}$ | $\Delta^2 \boldsymbol{u} = \boldsymbol{0}$ |
| **Green's functions** | $G(\boldsymbol{y},\boldsymbol{x}) = \begin{cases} -\frac{1}{4\pi r}, & d=3, \\ \frac{1}{2\pi}\log(r), & d=2. \end{cases}$ | $\mathcal{K}(\boldsymbol{x},\boldsymbol{y}) = \begin{cases} \frac{a-b}{r}\boldsymbol{I} + \frac{b}{r^3}\boldsymbol{r}\boldsymbol{r}^t, & d=3, \\ (b-a)\log(r)\boldsymbol{I} + \frac{b}{r^2}\boldsymbol{r}\boldsymbol{r}^t, & d=2. \end{cases}$ | $\begin{cases} G(\boldsymbol{y},\boldsymbol{x}) = -\frac{1}{4\pi r} \\ \bar{G}(\boldsymbol{y},\boldsymbol{x}) = -\frac{r}{8\pi} \end{cases}$ |
| **Boundary integral reformulation** | $\boldsymbol{u}(\boldsymbol{x}) = \int_{\partial\Omega} [\nabla_{\boldsymbol{n}} G(\boldsymbol{y},\boldsymbol{x})\boldsymbol{u}(\boldsymbol{y}) - G(\boldsymbol{y},\boldsymbol{x})\nabla_{\boldsymbol{n}}\boldsymbol{u}(\boldsymbol{y})]\, \mathrm{d}A_{\boldsymbol{y}}$ | $\boldsymbol{u}(\boldsymbol{x}) = \int_{\partial\Omega} [\mathcal{T}(\boldsymbol{y},\boldsymbol{x})\boldsymbol{u}(\boldsymbol{y}) + \mathcal{K}(\boldsymbol{y},\boldsymbol{x})\boldsymbol{\tau}(\boldsymbol{y})]\, \mathrm{d}A_{\boldsymbol{y}}$ | $\boldsymbol{u}(\boldsymbol{x}) = \int_{\partial\Omega} [\boldsymbol{u}(\boldsymbol{y})\nabla_{\boldsymbol{n}} G(\boldsymbol{y},\boldsymbol{x}) - G(\boldsymbol{y},\boldsymbol{x})\nabla_{\boldsymbol{n}}\boldsymbol{u}(\boldsymbol{y}) + \Delta\boldsymbol{u}(\boldsymbol{y})\nabla_{\boldsymbol{n}}\bar{G}(\boldsymbol{y},\boldsymbol{x}) - \bar{G}(\boldsymbol{y},\boldsymbol{x})\nabla_{\boldsymbol{n}}\Delta\boldsymbol{u}(\boldsymbol{y})]\, \mathrm{d}A_{\boldsymbol{y}}$ |

$$\boldsymbol{u}(\boldsymbol{x}) = \boldsymbol{x}$$

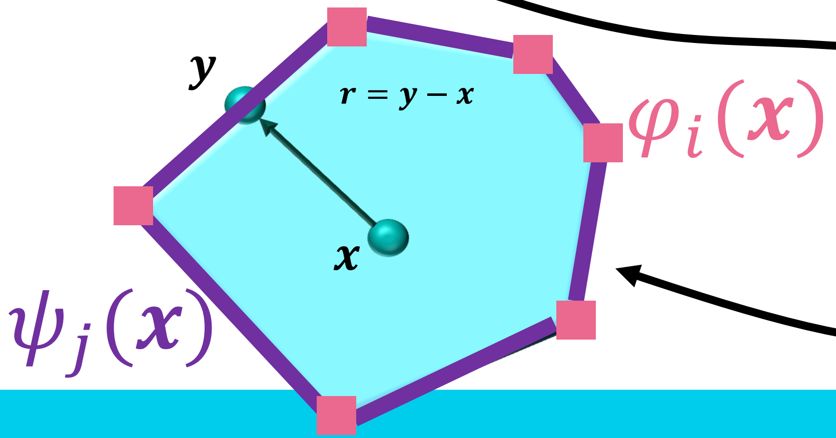

# GENERALIZED BARYCENTRIC COORDINATES WITH NORMAL CONTROL

SCA 2025

| | Green coordinates [Lipman et al. 2008] | Somigliana coordinates [Chen et al. 2023] | Biharmonic coordinates [Thiery et al. 2024] |
|---|---|---|---|
| **PDE** | $\Delta \boldsymbol{u} = \boldsymbol{0}$ | $\Delta \boldsymbol{u} + \frac{1}{1-2\nu}\nabla(\nabla \cdot \boldsymbol{u}) = \boldsymbol{0}$ | $\Delta^2 \boldsymbol{u} = \boldsymbol{0}$ |
| **Green's functions** | $G(\boldsymbol{y},\boldsymbol{x}) = \begin{cases} -\frac{1}{4\pi r}, & d=3, \\ \frac{1}{2\pi}\log(r), & d=2. \end{cases}$ | $\mathcal{K}(\boldsymbol{x},\boldsymbol{y}) = \begin{cases} \frac{a-b}{r}\boldsymbol{I} + \frac{b}{r^3}\boldsymbol{r}\boldsymbol{r}^t, & d=3, \\ (b-a)\log(r)\boldsymbol{I} + \frac{b}{r^2}\boldsymbol{r}\boldsymbol{r}^t, & d=2. \end{cases}$ | $\begin{cases} G(\boldsymbol{y},\boldsymbol{x}) = -\frac{1}{4\pi r} \\ \bar{G}(\boldsymbol{y},\boldsymbol{x}) = -\frac{r}{8\pi} \end{cases}$ |
| **Boundary integral reformulation** | $\boldsymbol{u}(\boldsymbol{x}) = \int_{\partial\Omega} [\nabla_{\boldsymbol{n}} G(\boldsymbol{y},\boldsymbol{x})\boldsymbol{u}(\boldsymbol{y}) - G(\boldsymbol{y},\boldsymbol{x})\nabla_{\boldsymbol{n}}\boldsymbol{u}(\boldsymbol{y})]\,\mathrm{d}A_{\boldsymbol{y}}$ | $\boldsymbol{u}(\boldsymbol{x}) = \int_{\partial\Omega} [\mathcal{T}(\boldsymbol{y},\boldsymbol{x})\boldsymbol{u}(\boldsymbol{y}) + \mathcal{K}(\boldsymbol{y},\boldsymbol{x})\boldsymbol{\tau}(\boldsymbol{y})]\,\mathrm{d}A_{\boldsymbol{y}}$ | $\boldsymbol{u}(\boldsymbol{x}) = \int_{\partial\Omega} [\boldsymbol{u}(\boldsymbol{y})\nabla_{\boldsymbol{n}} G(\boldsymbol{y},\boldsymbol{x}) - G(\boldsymbol{y},\boldsymbol{x})\nabla_{\boldsymbol{n}}\boldsymbol{u}(\boldsymbol{y}) + \Delta\boldsymbol{u}(\boldsymbol{y})\nabla_{\boldsymbol{n}}\bar{G}(\boldsymbol{y},\boldsymbol{x}) - \bar{G}(\boldsymbol{y},\boldsymbol{x})\nabla_{\boldsymbol{n}}\Delta\boldsymbol{u}(\boldsymbol{y})]\,\mathrm{d}A_{\boldsymbol{y}}$ |
| | Conformal mapping | Elastic effects, e.g., volume preserving and natural bulges | High-order smoothness. More space to incorporate boundary conditions |

# SPECIFYING BOUNDARY CONDITIONS

SCA2025

- When the cage is deformed, i.e., with new specified vertex positions

$$\tilde{\boldsymbol{x}}(\boldsymbol{x}) = \sum_i \varphi_i(\boldsymbol{x})\tilde{\boldsymbol{v}}_i \quad + \sum_k \psi_k(\boldsymbol{x})[?]$$

- In BEM, the normal control part is $\partial_{\boldsymbol{n}}\tilde{\boldsymbol{x}}|_{\partial\Omega}$ solved from $\tilde{\boldsymbol{x}}|_{\partial\Omega}$
  - Dirichlet and Neumann boundary conditions are compatible
- In cage deformation, there is no golden standard so we just **“guess”** the boundary normal derivatives
  - Efficient for real-time manipulation
  - Parameterize Neumann conditions to support flexible control over the interior deformation
- Price to pay: normal terms are not compatible with cage vertex positions
  - Consequently, the interior deformation could be not following the cage tightly

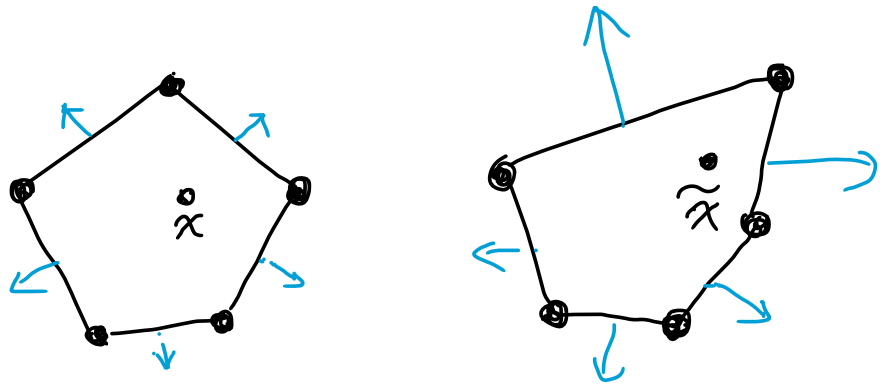

undeformed    deformed

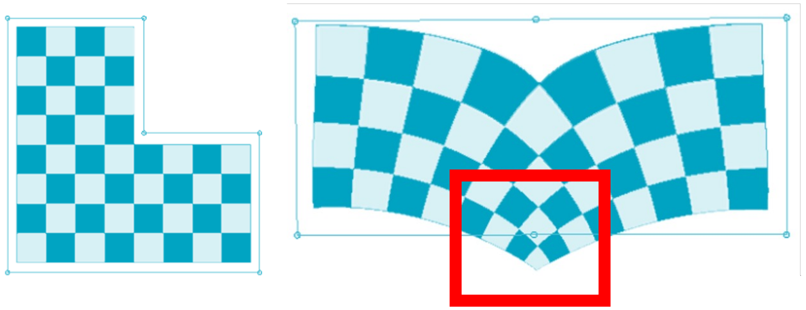

# CONTROLLING BOUNDARY STRETCHING



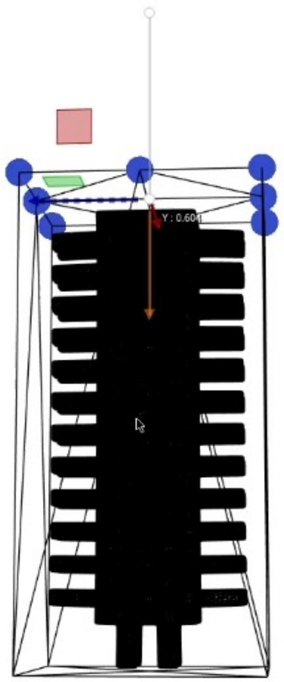

Small bulge

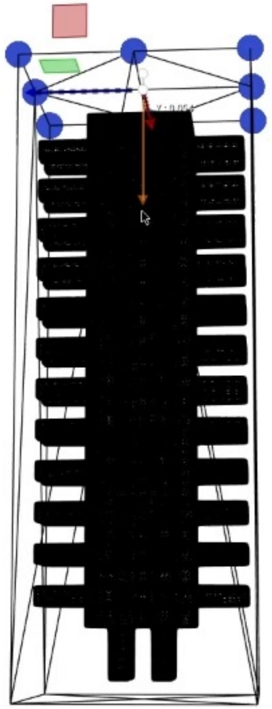

Large bulge

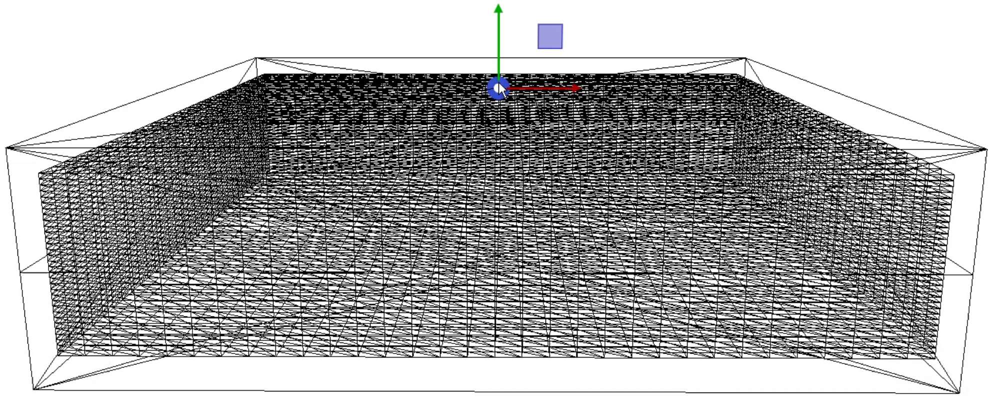

Large bulge

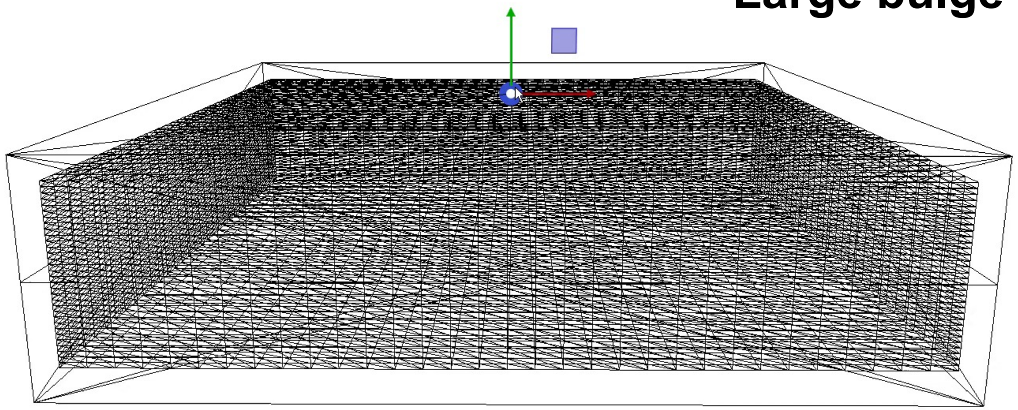

Small bulge

# CONTROLLING BOUNDARY ROTATIONS

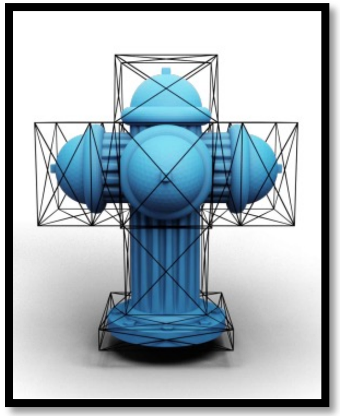

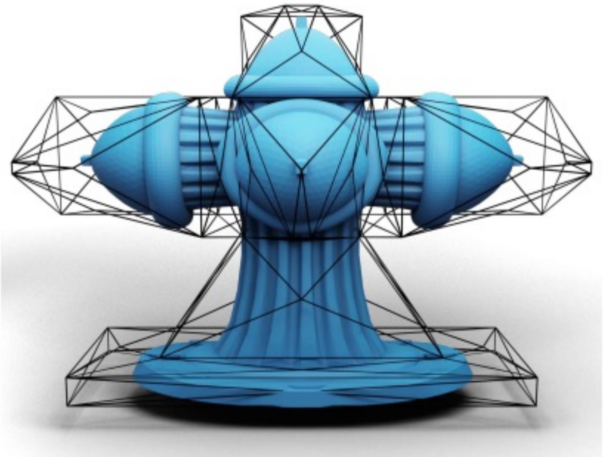

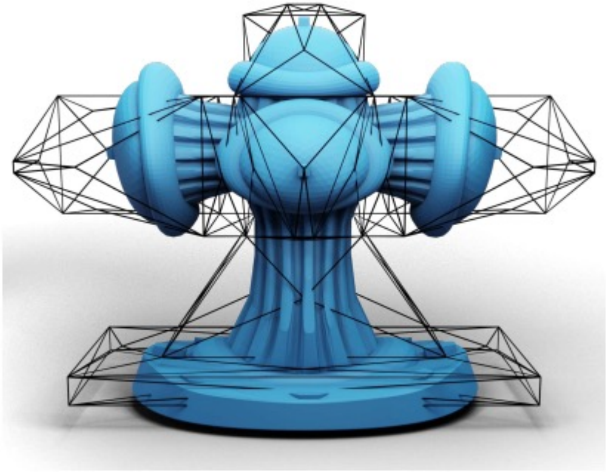

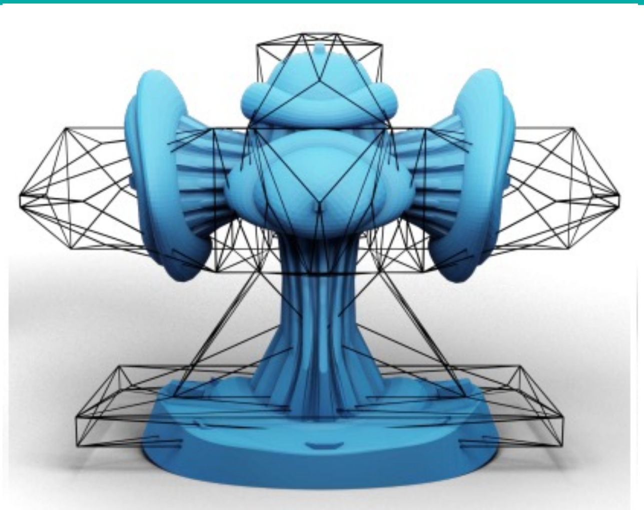

## Rest pose

## Global variant

$R_k = R_{global,}\ \lambda_k = \lambda_{global}$ from the optimal similarity transformation

## In between

blend global and local $R_k, \lambda_k$

## Local variant

$R_k$ and $\lambda_k$ are decuded on per facet basis

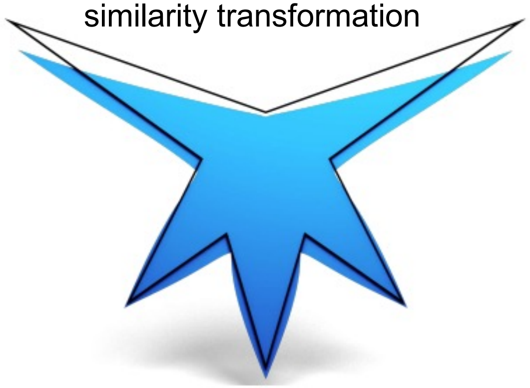

# UNFOLDING THE POWER OF GREEN'S FUNCTIONS

SCA 2025

$$u(x) = \int G(y,x)g(y)dS_y$$

**PARAMETERIZATION** of the fundamental solutions to **general** linear operators

$$s.t.\ \mathcal{D}(u)|_{\partial\Omega} = u_0$$

**SCALABILITY** of enforcing boundary conditions for **large-scale** problems

- Free-space shape editing
  - Enrich the expressiveness of Green's functions
- Scalable BEM solvers
  - Leverage the inherent smoothness of the Green's function for efficient inverse approximation
- Cage-based deformation
  - Explore the space of weighting to combine Green's functions for rich geometries in real-time

$$x = Gw$$

$$w = G^{-1}x$$

$$x = Gw$$

# Thank you!